# UC Berkeley

## UC Berkeley Previously Published Works

### Title

Arbuscular mycorrhiza convey significant plant carbon to a diverse hyphosphere microbial food web and mineral-associated organic matter

### Permalink

https://escholarship.org/uc/item/56k7r0x5

### Journal

New Phytologist, 242(4)

### ISSN

0028-646X

### Authors

Kakouridis, Anne
Yuan, Mengting
Nuccio, Erin E
et al.

### Publication Date

2024-05-01

### DOI

10.1111/nph.19560

### Copyright Information

This work is made available under the terms of a Creative Commons Attribution License, available at https://creativecommons.org/licenses/by/4.0/

Peer reviewed

eScholarship.org Powered by the California Digital Library
University of California

Check for updates

New Phytologist

Research

# Arbuscular mycorrhiza convey significant plant carbon to a diverse hyphosphere microbial food web and mineral-associated organic matter

**Anne Kakouridis[1,2], Mengting Yuan[1], Erin E. Nuccio[3], John A. Hagen[1], Christina A. Fossum[1], Madeline L. Moore[1,2], Katerina Y. Estera-Molina[1,3], Peter S. Nico[2], Peter K. Weber[3], Jennifer Pett-Ridge[3,4] and Mary K. Firestone[1]**

[1]University of California Berkeley, Berkeley, CA 94720, USA; [2]Lawrence Berkeley National Laboratory, Berkeley, CA 94720, USA; [3]Lawrence Livermore National Laboratory, Livermore 94550 CA, USA; [4]University of California Merced, Merced 95343 CA, USA

Authors for correspondence:
*Mary K. Firestone*
*Email: mkfstone@berkeley.edu*

*Anne Kakouridis*
*Email: annekakouridis@berkeley.edu*

Received: *8 July 2023*
Accepted: *4 December 2023*

*New Phytologist* (2024)
**doi**: 10.1111/nph.19560

**Key words:** $^{13}$C SIP, arbuscular mycorrhizal fungi, hyphosphere, plant–soil–microbe interactions, soil carbon, soil food web, soil organic matter, stable isotopes.

## Summary

- Arbuscular mycorrhizal fungi (AMF) transport substantial plant carbon (C) that serves as a substrate for soil organisms, a precursor of soil organic matter (SOM), and a driver of soil microbial dynamics. Using two-chamber microcosms where an air gap isolated AMF from roots, we $^{13}CO_2$-labeled *Avena barbata* for 6 wk and measured the C *Rhizophagus intraradices* transferred to SOM and hyphosphere microorganisms.
- NanoSIMS imaging revealed hyphae and roots had similar $^{13}$C enrichment. SOM density fractionation, $^{13}$C NMR, and IRMS showed AMF transferred 0.77 mg C g$^{-1}$ of soil (increasing total C by 2% relative to non-mycorrhizal controls); 33% was found in occluded or mineral-associated pools.
- In the AMF hyphosphere, there was no overall change in community diversity but 36 bacterial ASVs significantly changed in relative abundance. With stable isotope probing (SIP)-enabled shotgun sequencing, we found taxa from the Solibacterales, Sphingobacteriales, Myxococcales, and Nitrososphaerales (ammonium oxidizing archaea) were highly enriched in AMF-imported $^{13}$C (> 20 atom%). Mapping sequences from $^{13}$C-SIP metagenomes to total ASVs showed at least 92 bacteria and archaea were significantly $^{13}$C-enriched.
- Our results illustrate the quantitative and ecological impact of hyphal C transport on the formation of potentially protective SOM pools and microbial roles in the AMF hyphosphere soil food web.

## Introduction

Arbuscular mycorrhizal fungi (AMF, phylum Mucoromycota, subphylum Glomeromycotina) form symbiotic associations with over 80% of vascular plant families (Schüßler *et al.*, 2001; Spatafora *et al.*, 2016) and facilitate plant nutrient uptake in exchange for photosynthetically derived carbon (C) (Smith & Read, 2008; Willis *et al.*, 2013). Arbuscular mycorrhizal fungi consume 6.2% of plant photosynthate C on average (Hawkins *et al.*, 2023) and grow extensive hyphal networks into soil (Jakobsen & Rosendahl, 1990; Tome *et al.*, 2015), which can account for 15–30% of the soil microbial biomass (Leake *et al.*, 2004; Parniske, 2008; Qin *et al.*, 2017), and explore a soil volume substantially larger than fine roots alone (See *et al.*, 2022). The composition, exudates, and interactions of AMF hyphae with plant roots and soil microbes play a critical and complex role in soil C processes (Wei *et al.*, 2019; Domeignoz-Horta *et al.*, 2021; Horsch *et al.*, 2023). While soil C dynamics have been the focus of substantial research, gaps remain in our knowledge of the magnitude and fate of C fluxes within the mycorrhizal pathway (Sulman *et al.*, 2018; Domeignoz-Horta *et al.*, 2021) and how surrounding soil biota are affected.

Plant-fixed C, distributed into soil as root biomass, mycorrhizal tissues, and their exudates, is the primary source of soil organic C and is transformed into soil organic matter (SOM) through diverse chemical and microbial processes (Torn *et al.*, 1997; Trumbore, 2000; Schmidt *et al.*, 2011). Since SOM holds not only organic C but also water and nutrients, its persistence is a major goal in climate change mitigation and sustainable land management. The mechanisms responsible for SOM persistence are complex and under active investigation (Jastrow *et al.*, 2007; Treseder, 2016; Dynarski *et al.*, 2020; Lehmann *et al.*, 2020). Amidst the paths between plant photosynthate and SOM, AMF hyphae and soil microorganisms serve as primary intermediaries; their biomass and residues can contribute to slow-cycling and persistent forms of C that may become occluded within aggregates or associated with mineral surfaces (Miller & Jastrow, 2000; Dynarski *et al.*, 2020; Angst *et al.*, 2021; See *et al.*, 2022). While occluded and mineral-associated soil C is not always more persistent due to potential desorption (Keiluweit *et al.*, 2015; Li *et al.*,

© 2024 The Authors
*New Phytologist* © 2024 New Phytologist Foundation
This is an open access article under the terms of the Creative Commons Attribution-NonCommercial License, which permits use, distribution and reproduction in any medium, provided the original work is properly cited and is not used for commercial purposes.

2021), this C does typically have longer turnover times than other soil pools (Heckman *et al.*, 2022).

Several methods can distinguish C present as aggregate-occluded or mineral-associated C-forms. In the 'density fraction' approach, SOM is partitioned based on density into soil fractions that are operationally defined: particulate organic matter (free light fraction or light fraction), occluded within soil aggregates (occluded light fraction or occluded fraction), and mineral-associated (heavy fraction; Sollins *et al.*, 2006, 2009). Organic C in these soil fractions has distinct rates of biochemical and microbial degradation (Sollins *et al.*, 2006, 2009), and these fractions are widely thought to represent ecologically relevant soil components (Moni *et al.*, 2010; Hatton *et al.*, 2012) shaped by climate and ecosystem type (Sokol *et al.*, 2022).

Arbuscular mycorrhizal fungi may alter the relative distribution of organic C in different soil fractions (Orwin *et al.*, 2011; Soudzilovskaia *et al.*, 2015, 2019; Cheeke *et al.*, 2016; Frey, 2019) and thereby influence the persistence of C in soil. Arbuscular mycorrhizal fungi have been shown to increase (Treseder, 2016; Wang *et al.*, 2016; Zhang *et al.*, 2020) or decrease (Hodge *et al.*, 2001; Cheng *et al.*, 2012; Herman *et al.*, 2012; Paterson *et al.*, 2016; Frey, 2019) soil C accumulation depending on the study system, environmental variables, and time frame. Arbuscular mycorrhizal fungi respire C and can lead to an increase in decomposition and soil respiration (Hodge *et al.*, 2001; Cheng *et al.*, 2012; Lang *et al.*, 2021), reducing the amount of C available for SOM formation. Yet, AMF can promote soil C accumulation by increasing the formation of soil aggregates (Rillig *et al.*, 2001b; Wilson *et al.*, 2009; Leifheit *et al.*, 2015) and SOM–mineral associations (Smits *et al.*, 2009; See *et al.*, 2022), and thereby protect organic C from decomposition. Arbuscular mycorrhizal fungi directly contribute C to SOM formation, as their cell materials become components of SOM when they senesce and are degraded (Kögel-Knabner, 2002; Langley & Hungate, 2003; Godbold *et al.*, 2006). Arbuscular mycorrhizal fungi hyphae also release C compounds into surrounding soil (hyphosphere) as exudates (Hooker *et al.*, 2007; Toljander *et al.*, 2007) that can be transferred to other microbes (Herman *et al.*, 2012; Kaiser *et al.*, 2015; Bunn *et al.*, 2019).

The presence of AMF may quantitatively and qualitatively alter soil bacterial communities, and AMF hyphae and spores provide important niches for bacterial interactions and growth. Bacteria can colonize living hyphae (Toljander *et al.*, 2006, 2007) and form biofilms on hyphal surfaces (Lecomte *et al.*, 2011), consume hyphal exudates (Kaiser *et al.*, 2015), and help AMF mobilize nutrients in soil (Jiang *et al.*, 2021). Bacteria can also attach to non-living hyphae and use them as a substrate (Toljander *et al.*, 2006, 2007). Our prior work suggests AMF have diverse effects on nearby hyphosphere microbiomes: stimulating organic matter decomposition and nitrogen (N) transfer (Nuccio *et al.*, 2013), supporting water transport (Kakouridis *et al.*, 2022) and drought resilience (Hestrin *et al.*, 2022), and stimulating cross-kingdom trophic interactions (Nuccio *et al.*, 2022). However, these small-scale interactions can be difficult to directly measure, and under native soil conditions, it is particularly challenging to directly evaluate the hyphosphere effects without the influence of roots and rhizosphere organisms.

Arbuscular mycorrhizal fungi represent a globally important pathway for the flow of C from plants into soil (Hawkins *et al.*, 2023), yet it remains unclear how AMF and their hyphosphere microbiome influence the initial incorporation of organic C into soil, separately from roots. In this study, we used $^{13}C$ stable isotope tracing and molecular techniques to measure C transfer into soil, from the host plant *Avena barbata*, a widespread annual grass, via the AMF *Rhizophagus intraradices*. In a glasshouse experiment, we used a two-compartment microcosm design to isolate AMF transfer of C into soil. To assess how AMF affect the short-term fate of plant-derived C, we used nanoscale secondary ion mass spectrometry (NanoSIMS) imaging and isotope ratio mass spectrometry (IRMS) to track $^{13}C$ after it was fixed by host plants and transferred by AMF into soil during 6 wk of exponential phase plant growth. Using soil from the no-plant compartment, we characterized the form of AMF-contributed C by density fractionation into light fraction (likely still free hyphae), occluded fraction (contained within aggregate structures), and heavy fraction (mineral-associated) pools. Changes in C chemistry were assessed by $^{13}C$ nuclear magnetic resonance (NMR) spectroscopy of soil aggregates. We also investigated the influence of AMF on hyphosphere soil microbial communities (independently from roots) by amplicon sequencing soil DNA and identifying the key microbial consumers of hyphal-derived C via stable isotope probing (SIP)-enabled metagenomic sequencing.

## Materials and Methods

### Experimental setup

Our experimental setup is described in detail in Kakouridis *et al.* (2022). In brief, three 2-wk-old *A. barbata* Pott ex Link seedlings were planted in the 'plant compartment' of two-compartment microcosms (10 × 2.5 × 26.5 cm; Fig. 1a), which was separated from the 'no-plant compartment' by a 3.2-mm air gap to prevent liquid water from traveling passively between compartments. Both sides of the air gap had nylon mesh, either 18 µm (allowing hyphae but excluding roots) or 0.45 µm (excluding both hyphae and roots). A total of 24 microcosms were used, 18 with 18 µm mesh, and six with 0.45 µm mesh. The plant compartment was packed with a 1 : 1 sand–clay mixture to a 1.21 g $cm^{-3}$ density (referred to as the 'sand mix'). The no-plant compartment (10 × 1 × 26.5 cm) was packed with a 1 : 1 soil–sand mixture to a 1.21 g $cm^{-3}$ density (referred to as the 'soil mix') using field-collected soil containing live microbial communities. This soil (0–10 cm) was collected at the Hopland Research and Extension Center (38°59′35″N, 123°4′3″W) from a site where *A. barbata* was the dominant vegetation. Collected soil was air-dried, sieved (2 mm) to remove rocks and litter, and kept in a 4°C cold room before being mixed with sand and packed into the microcosms.

In the plant compartment, the sand mix was inoculated with 26 g of *R. intraradices* (N.C. Schenck & G.S. Sm.) C. Walker & A. Schuessler 2010 whole inoculum (accession no. AZ243, International Culture Collection of (Vesicular) Arbuscular Mycorrhizal Fungi (INVAM), The University of Kansas, Lawrence, KS, USA). *Rhizophagus intraradices* was selected because it naturally



© 2024 The Authors
*New Phytologist* © 2024 New Phytologist Foundation

14698137, 0, Downloaded from https://nph.onlinelibrary.wiley.com/doi/10.1111/nph.19560, Wiley Online Library on [03/04/2024]. See the Terms and Conditions (https://onlinelibrary.wiley.com/terms-and-conditions) on Wiley Online Library for rules of use; OA articles are governed by the applicable Creative Commons License

14698137, 0, Downloaded from https://nph.onlinelibrary.wiley.com/doi/10.1111/nph.19560, Wiley Online Library on [03/04/2024]. See the Terms and Conditions (https://onlinelibrary.wiley.com/terms-and-conditions) on Wiley Online Library for rules of use; OA articles are governed by the applicable Creative Commons License

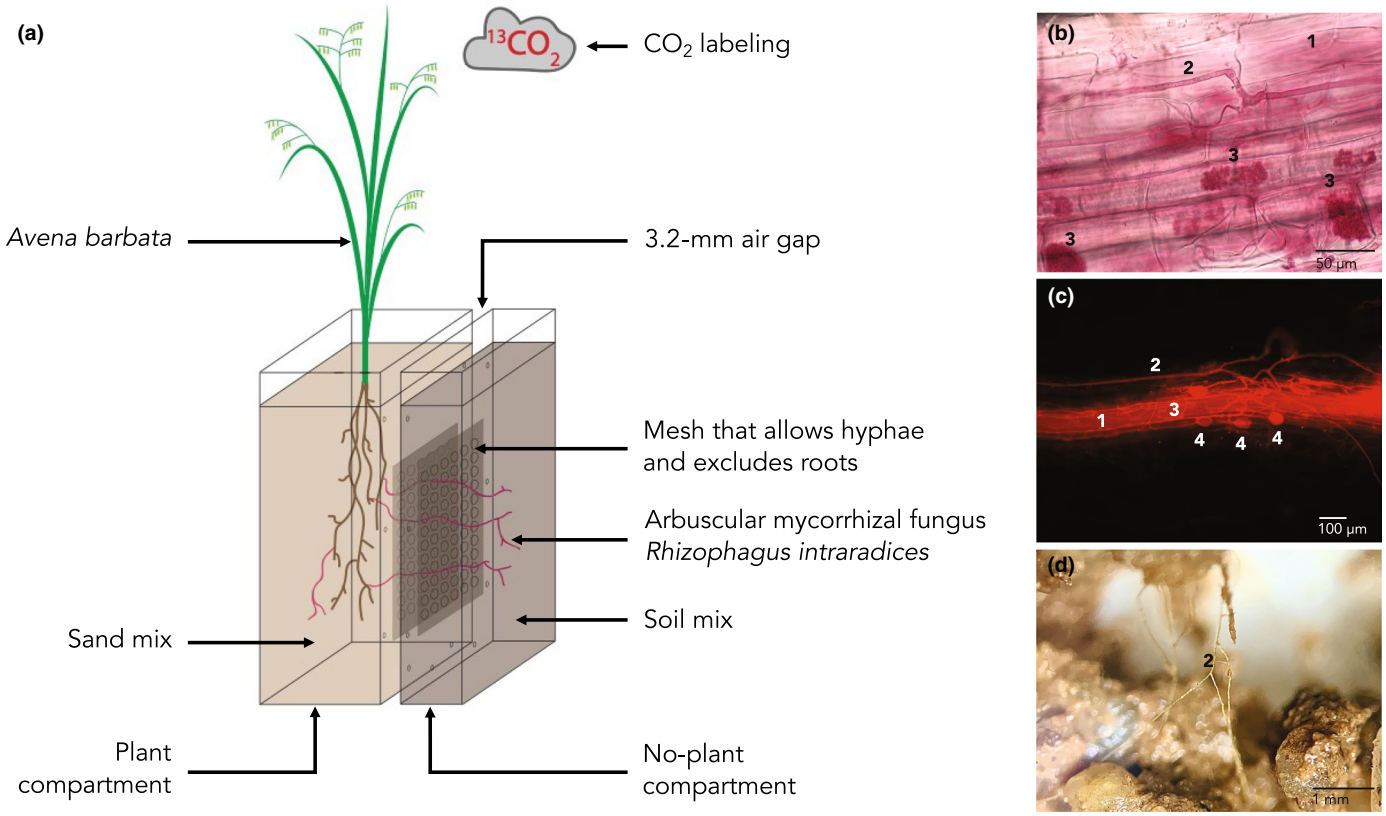


**Fig. 1** Arbuscular mycorrhizal fungus (AMF) *Rhizophagus intraradices*, inoculated within the plant compartment, colonized roots of the host plant *Avena barbata* and grew across an air gap to reach the no-plant compartment. (a) Our experimental design tested for the movement of plant carbon (C) into root-free soil via AMF hyphae. This figure shows an AMF-permitted $^{13}C$ microcosm ('+AMF') where plants were grown in a 99 atom% $^{13}CO_2$ atmosphere in Weeks 5–10 and AMF were able to access a no-plant compartment by crossing a 3.2-mm air gap (through a mesh with 18-µm pore size). Two other treatments included as follows: (1) AMF-excluded $^{13}C$ controls ('−AMF') where plants were grown in a $^{13}CO_2$ atmosphere in Weeks 5–10, but AMF were not able to access the no-plant compartment because the mesh (0.45-µm pore size) between the compartments restricted both roots and hyphae from crossing from the plant compartment; and (2) AMF-permitted $^{12}C$ controls ('$^{12}C$'), where plants were grown in an ambient $CO_2$ atmosphere in Weeks 5–10 and AMF were able to access the no-plant compartment. All microcosms experienced an ambient $CO_2$ atmosphere in Weeks 1–4. Plants were harvested at the end of Week 10. In sum, the experiment included 12 +AMF microcosms, six −AMF microcosms, and six $^{12}C$ microcosms. (b, c) *Avena barbata* roots stained with acid fuchsin showing AMF structures. (b) Bright field micrographs. (c) Fluorescence images at wavelengths $\lambda_{ex}$ 596 nm and $\lambda_{em}$ 615 nm, which target AMF. (d) Soil–sand mixture from the no-plant compartment of a +AMF microcosm with AMF hyphae visible under a dissecting microscope. In (b–d): 1, Root; 2, Hypha; 3, Arbuscule; 4, Vesicle.

colonizes *A. barbata* roots at the field site where seeds and soil were collected for this experiment (Kakouridis, 2021). Bone meal (78 mg) was mixed into the plant compartment to encourage AMF establishment, and into the no-plant compartment to act as a bait for AMF to cross the air gap (Supporting Information Table S1).

The microcosms were incubated in growth chambers in the Environmental Plant Isotope Chamber (EPIC) facility, located in the Oxford Tract Greenhouse at UC Berkeley, where environmental conditions were monitored and controlled. Three chambers were used, with eight microcosms in each, organized in a randomized fashion. Volumetric water content was monitored with electronic probes (EC-5; Decagon Services, Pullman, WA, USA), and maintained at *c.* 17% by watering three times weekly with autoclaved distilled water in both compartments. Ten milliliters of filter-sterilized Rorison's nutrient solution (Rorison & Rorison, 1987) was added to the plant compartment (low P) and no-plant compartment (high P) once per week (Table S1). The plant compartment of microcosms with 0.45 µm mesh received twice as much nutrient solution as microcosms with 18 µm mesh, to make up for the nutrients plants could obtain via AMF from the no-plant compartment (Table S1).

Twelve microcosms with 18 µm mesh (AMF-permitted $^{13}C$ microcosms, termed '+AMF') and six microcosms with 0.45 µm mesh (AMF-excluded $^{13}C$ microcosms, termed '−AMF') were placed in a $^{13}C$-labeled $CO_2$ atmosphere during Weeks 5–10. The remaining six microcosms with 18 µm mesh (AMF-permitted $^{12}C$ microcosms, termed '$^{12}C$') remained in a natural abundance $CO_2$ atmosphere for the full 10 wk.

## Harvest and sample processing

At the end of Week 10, all microcosms were destructively sampled. Shoots were cut at the base, dried at 60°C, and weighed for aboveground biomass (Table S1). Roots were gently harvested and divided into three aliquots so that each aliquot contained a

© 2024 The Authors
*New Phytologist* © 2024 New Phytologist Foundation

randomized subsample of roots representing one-third of the root system: (1) To confirm AMF colonization under the microscope, roots were placed in distilled water for staining with acid fuchsin, (2) to confirm AMF presence by DNA sequencing, roots were placed in cell release buffer for molecular analysis (Brodie *et al.*, 2011), and (3) to assess the $^{13}C$ enrichment via IRMS and to measure belowground biomass, roots were placed in paper envelopes and dried at 60°C (Table S1).

The sand mix and soil mix were collected and split into several aliquots: (1) 10 g for gravimetric water content was oven-dried at 105°C (Table S1) and (2) samples for molecular analysis were flash frozen in liquid nitrogen and stored at −80°C. In addition, the soil mix was preserved for hyphal extraction by storing at 4°C and for soil density fractionation by air drying.

Hyphae evident in the air gap were collected on the mesh facing the inside of the air gap using tweezers and placed into tubes for DNA extraction the same day. Visible hyphae were also collected from the plant and no-plant compartments of each microcosm using a dissecting scope and tweezers, then placed on silica wafers covered with carbon sticky tape for scanning electron microscopy (SEM) and NanoSIMS.

### Microscopy

To observe and confirm AMF colonization under the microscope, roots were stained with acid fuchsin using a protocol modified from Habte & Osorio (2001) and described in Kakouridis *et al.* (2022). Stained roots were mounted on slides and observed under both bright field and fluorescence ($\lambda_{ex}$ 596 nm/$\lambda_{em}$ 615 nm).

### Molecular methods

To extract AMF spores and hyphae from the sand and soil mix, and then extract DNA from roots, soil mix, spores, and hyphae, we followed methods described in Kakouridis *et al.* (2022). In brief, we used a cell release buffer (Brodie *et al.*, 2011) to remove surface microbial cells from roots, hexametaphosphate to separate out AMF spores and hyphae, and conducted DNA extraction from roots, spores, hyphae, and soil mix with a DNeasy PowerSoil kit (Qiagen). To collect hyphosphere microbial communities, hyphae with soil attached were picked using tweezers under a dissecting microscope.

DNA extracted from roots, soil mix, spores and hyphae, and hyphosphere microbial communities was quantified with the Quant-iT™ PicoGreen™ dsDNA Assay Kit (Invitrogen), and concentrations were normalized to 5 ng $\mu l^{-1}$. To identify the AMF present, PCR was conducted using WANDA (Dumbrell *et al.*, 2011) and AML2 (Lee *et al.*, 2008) primers according to procedures described in Kakouridis *et al.* (2022). A sequence was considered a match for *R. intraradices* if query coverage and percent identity were both > 97%.

DNA extracts were used for both amplicon and SIP-metagenome sequencing. To identify the bacteria present on hyphae and in hyphosphere soil, a sequencing library was prepared using a phasing amplicon technique (Wu *et al.*, 2015) on the normalized DNA samples from +AMF and −AMF soil mix from the no-plant compartment with 515F/806R primers (Caporaso *et al.*, 2012) targeting the 16S rRNA gene V4 region. The library was prepared in the Zhou laboratory at the University of Oklahoma and sequenced on the Illumina MiSeq platform with 2 × 250 bp paired-end format.

### 16S rRNA sequence processing

Amplicon sequences were processed with QIIME2 (Bolyen *et al.*, 2019). After demultiplexing, a total of 637 832 raw sequences were obtained from the six +AMF and six −AMF soil samples. After primer trimming, sequences were denoised using DADA2 (Callahan *et al.*, 2016) and clustered into amplicon sequence variants (ASVs). The representative sequences of each ASV were then used to assign taxonomy based on a classifier trained with the SILVA database (v.132-99-515-806). Amplicon sequence variants unassigned at the domain level or identified as mitochondria or chloroplast sequences were discarded. This resulted in 3019 ASVs in 12 samples, with 23 502–41 551 sequences per sample. The SRA sequence records are accessible with the following link: https://www.ncbi.nlm.nih.gov/sra/PRJNA1051335.

### $^{13}C$ DNA-SIP and metagenomic read processing

$^{13}C$ DNA-SIP and metagenomic sequencing of the fractionated DNA samples have been described previously by Nuccio *et al.* (2022). Briefly, 350 ng of $^{13}C$- and $^{12}C$-AMF DNA ($n = 3$) was added to SIP density gradients, ultracentrifuged, fractionated, precipitated, and quantified with Lawrence Livermore National Laboratory's high-throughput HT-SIP pipeline (Nuccio *et al.*, 2022).

After quality control, we retrieved 16S sequences from the SIP-metagenomics dataset by mapping the raw SIP-metagenome reads (14 fractions per gradient) to our 3019 16S amplicon ASVs using BBSPLIT (Bushnell, 2014); this strategy allowed us to identify $^{13}C$-enriched organisms that may not have assembled in our previous work (Nuccio *et al.*, 2022). Sequences were required to unambiguously map to a single ASV and mapped in 'semiperfect' mode, which requires a 100% sequence match (max index of 2) but allows N's and will allow a read to run off the end of the sequence. We generated an OTU table from the BBSPLIT ASV matches for each SIP fraction, and then calculated ASV atom percent excess (APE) using the QUANTITATIVE SIP (QSIP) pipeline (Hungate *et al.*, 2015; Koch *et al.*, 2018). We required an ASV be present in three replicates and at least three fractions. To determine whether an ASV was significantly enriched in $^{13}C$, we required the mean APE lower 90% confidence interval be significantly greater than zero, and the weighted average differences (WAD) of the $^{13}C$ and $^{12}C$ control density curves be significantly different ($P$-value < 0.05).

### Soil density fractionation

We used a soil density fractionation method described in Fossum *et al.* (2022), which was modified from Hicks Pries *et al.* (2018) and Strickland & Sollins (1987). In brief, 20 g of air-dried soil



© 2024 The Authors
*New Phytologist* © 2024 New Phytologist Foundation

14698137, 0, Downloaded from https://nph.onlinelibrary.wiley.com/doi/10.1111/nph.19560, Wiley Online Library on [03/04/2024]. See the Terms and Conditions (https://onlinelibrary.wiley.com/terms-and-conditions) on Wiley Online Library for rules of use; OA articles are governed by the applicable Creative Commons License

14698137, 0, Downloaded from https://nph.onlinelibrary.wiley.com/doi/10.1111/nph.19560, Wiley Online Library on [03/04/2024]. See the Terms and Conditions (https://onlinelibrary.wiley.com/terms-and-conditions) on Wiley Online Library for rules of use; OA articles are governed by the applicable Creative Commons License

mix and 50 ml of sodium polytungstate (SPT; Geoliquids) were prepared to a density of 1.75 g $cm^{-3}$, centrifuged at 3700 ***g***, and left to settle. Particles floating on top were defined as the light fraction. The light fraction was aspirated onto a 0.8-μm glass microfiber filter (Whatman, Cytiva, Marlborough, MA, USA), rinsed with Milli-Q water, and then dried at 55°C and weighed. To collect the occluded fraction, the remaining soil–SPT mixture was shaken with a benchtop mixer for 1 min, sonicated for 90 s, allowed to settle, and then centrifuged for 1 h. The occluded fraction was then removed by aspiration, dried, and weighed. The remaining sediment ($\rho > 1.75$ g $cm^{-3}$) was defined as the heavy fraction. One hundred and fifty milliliters of Milli-Q water was added, vigorously shaken by hand, and then centrifuged for 20 min. The supernatant was aspirated and discarded. This process was repeated five times, or until the density of the supernatant reached 1 g $cm^{-3}$. The heavy fraction was transferred, dried, and weighed in the same manner as the light and occluded fractions. After drying, all fractions were ground to a fine powder.

### $^{13}C$ isotope ratio mass spectrometry (IRMS)

Samples of shoots, roots, sand mix, soil mix, and soil fractions were finely ground, weighed, and analyzed for total C and $^{13}C$ abundance by dry combustion on a PDZ Europa ANCA-GSL elemental analyzer interfaced to a PDZ Europa 20-20 isotope ratio mass spectrometer (Sercon Ltd, Cheshire, UK) with a precision for $^{13}C$ measurements of 0.1 per mil.

### Nanoscale secondary ion mass spectrometry (NanoSIMS)

To measure the atom% $^{13}C$ of hyphae, mounted hyphae collected from the plant compartment, air gap, and no-plant compartment were coated with gold and mapped with an SEM (Inspect F; FEI, Hillsboro, OR, USA). The isotopic composition of the hyphae was measured by NanoSIMS (NanoSIMS 50; CAMECA, Gennevilliers, France). We collected a total of 150 analysis regions (30 μm by 30 μm) to gain a broad survey of the distribution of $^{13}C$ enrichment in hyphae. Each location was first sputtered with a *c.* 60 pA $Cs^+$ beam to a depth of *c.* 60 nm to enhance the yield of negative secondary ions and reach sputtering equilibrium (stable secondary ion counts; Ghosal *et al.*, 2008). Then, a 2 pA $Cs^+$ beam with a nominal spot size of 200 nm was used to raster the analysis area with 256 × 256 pixels with 20–30 scans per sample. Five masses were collected as follows: $^{16}O^-$, $^{12}C_2^-$, $^{12}C^{13}C^-$, $^{12}C^{14}N^-$, and $^{31}P^-$ using electron multipliers and a mass resolving power *c.* 7000 (1.5× correction; Pett-Ridge & Weber, 2021). *Pseudomonas stutzerii* cells with known isotopic composition (previously analyzed by IRMS) were used as standards.

Images were processed using the L'IMAGE software (L.R. Nittler, www.limagesoftware.net). Images were corrected for deadtime and drift. Regions of interest (ROIs) were selected by first identifying hyphal structures from SEM and secondary electron imaging, and then based on areas of relatively uniform $^{13}C$ enrichment from ratio images of $^{12}C^{13}C^-$ : $^{12}C_2^-$. Areas of high $O^-$ counts (marker for minerals) were avoided. A total of 150 images were taken, from which a subset of 37 images with little charging and low $O^-$ counts were selected for calculations of hyphae atom% $^{13}C$.

### Solid-state $^{13}C$ nuclear magnetic resonance (NMR) spectroscopy

For +AMF microcosms and −AMF microcosms, hand-picked dried soil aggregate samples were finely ground. For logistical reasons, we were limited to running only six total samples for this method. To accommodate this limitation, the biological replicates were combined in pairs in order to reduce the number of samples to three for the +AMF microcosms and three for the −AMF microcosms. 1–100 mg of each of the six pooled samples were analyzed on a 500 MHz Bruker Avance-I Spectrometer (Bruker, Billerica, MA, USA) at the UC Davis NMR Facility as follows: MAS spinning speed 12 kHz, $^{13}C$-$^{1}H$ contact time 2 ms, relaxation delay time 1 s, number of scan 60 000–90 000 (signal-to-noise ratio: 15–20).

### Statistical analyses

Statistical analyses were conducted using R v.3.6.1 (R Core Team, 2017). A one-way analysis of variance (ANOVA) coupled with Fisher's least-significant difference (LSD) test (package AGRICOLAE, *P*-value adjustment using 'Holm') was used to differentiate means of atom% and the amount of $^{13}C$ from different treatments.

A paired Wilcoxon test was used to compare the average atom% $^{13}C$ of roots (IRMS) vs the average of hyphae NanoSIMS measurements from +AMF microcosms. One microcosm (#5) was excluded due to a technical issue with the hyphal sample preparation.

We calculated the alpha diversity (richness, Shannon index, and evenness, package VEGAN) and Faith's phylogenetic diversity (package PICANTE) of 16S rRNA detected prokaryotic communities (Kembel *et al.*, 2010; Oksanen *et al.*, 2019), and tested their differences between +AMF and −AMF treatments using a two-way ANOVA, treating 'chamber' as a random factor (and no significant chamber effect was observed). *P*-values were corrected using false discovery rate. The principal component analysis (package APE) and permutational multivariate analysis of variance (Adonis based on Bray–Curtis distance, package VEGAN) were performed to evaluate community composition difference among treatments. DESEQ analysis (Love *et al.*, 2014) was used to identify ASVs responding to the presence of AMF. To reduce potential noise in modeling fitting, we removed ASVs that only occurred in one of the six biological replicate samples under either +AMF or −AMF conditions. After this prevalence filtering, 1534 ASVs were included in the DESEQ analysis for parameter estimation and model fitting.

Through the manuscript, unless otherwise stated, we present 'mean ± standard error' where applicable.

## Results

### Confirmation of root colonization and hyphal networks in the no-plant compartment

Using WANDA-AML2 amplicon sequencing, we confirmed that roots of all microcosms were colonized by *R. intraradices*

© 2024 The Authors
*New Phytologist* © 2024 New Phytologist Foundation

and confirmed this AMF taxon in air gap hyphae and soil mix samples from +AMF and $^{12}C$ microcosms. We also observed hyphae, spores, and arbuscules in roots stained with acid fuchsin using light and fluorescence microscopy (Fig. 1b,c), confirming that *R. intraradices* was actively growing in roots over the course of our experiment. We observed hyphae crossing the air gap, and extensive hyphal networks in the no-plant compartment of +AMF and $^{12}C$ microcosms (Fig. 1d). In −AMF microcosms, we did not observe hyphae crossing the air gap nor hyphal networks in the soil mix.

## Confirmation of $^{13}C$ labeling and $^{13}C$ presence in no-plant compartment of +AMF microcosms

The atom% $^{13}C$ of shoots in +AMF and −AMF microcosms was 43.5 ± 1.5% and 43.7 ± 1.7%, respectively, and 1.1 ± 0.001% in $^{12}C$ microcosms (Fig. S1; Table S1). Root enrichment was 41.3 ± 1.9 atom% and 42.2 ± 2.0 atom% in +AMF and −AMF microcosms, respectively, and 1.1 ± 0.002% in $^{12}C$ microcosms (Fig. S1; Table S1). The atom% $^{13}C$ of the sand mix (plant compartment) was 5.3 ± 0.4% and 4.2 ± 0.2% in +AMF and −AMF microcosms, respectively, and 1.1 ± 0.003% in $^{12}C$ microcosms (Fig. S1; Table S1). The soil mix (no-plant compartment) of +AMF microcosms was significantly more $^{13}C$ enriched than that of −AMF and $^{12}C$ microcosms (atom% $^{13}C$ 1.8 ± 0.1% vs 1.1 ± 0.001% and 1.1 ± 0.0003%, respectively, $P < 0.001$; Fig. S1; Table S1). These results confirm there was significantly more $^{13}C$ in the no-plant compartment of +AMF microcosms and that the no-plant compartments of −AMF microcosms were not contaminated by $^{13}C$. The presence of AMF did not change soil gravimetric water content, aboveground biomass, root : shoot ratio, shoot C : N ratio and %N, but significantly increased plant P content and decreased plant N : P ratio (Table S1; Kakouridis *et al.*, 2022).

## $^{13}C$ in light, occluded, and heavy fractions of SOM

Soil organic matter from the soil mix (no-plant compartment) was separated into light, occluded and heavy fractions using a sodium polytungstate density gradient approach. Based on $^{13}C$ IRMS analysis of these density fractions, after 6 wk of labeling, 26.7 ± 3.0 mg of new $^{13}C$ was present in the no-plant compartment soil mix of +AMF microcosms (Fig. 2a; Tables S1, S2). This represents 74.4 mg C, which is equivalent to 0.77 mg C $g^{-1}$ of the native soil material (not including the sand) or 2.05% of the total C in the soil mix in the no-plant compartment (Methods S1).

The 26.7 mg of newly added $^{13}C$ found in the soil mix was distributed amongst the density fractions as follows: 17.8 mg $^{13}C$ (representing 49.6 mg total C or 1.37% of the total soil mix C) in the light fraction, 2.2 mg $^{13}C$ (representing 6.1 mg C or 0.17% of the total soil C) in the occluded fraction, and 6.7 mg $^{13}C$ (representing 18.7 mg C or 0.52% of the total soil C) in the heavy fraction (Fig. 2b).

## Hyphae highly enriched with $^{13}C$

To determine the average $^{13}C$ enrichment of hyphae, we collected NanoSIMS images of hyphae from the plant compartment, air gap, and no-plant compartment of +AMF microcosms (Fig. 3a–e). Based on an average of 37 images, hyphae were 35.9 ± 1.5% $^{13}C$ enriched (Fig. 3f; Table S3). A paired Wilcoxon test between five matched roots and hyphae samples indicated no statistical difference between the enrichment of roots and hyphae ($P = 0.063$; Fig. 3f).

## NMR spectra suggest carbohydrates in the presence of AMF

$^{13}C$-NMR spectra were obtained for six soil mix samples (three from +AMF microcosms and three from −AMF microcosms;

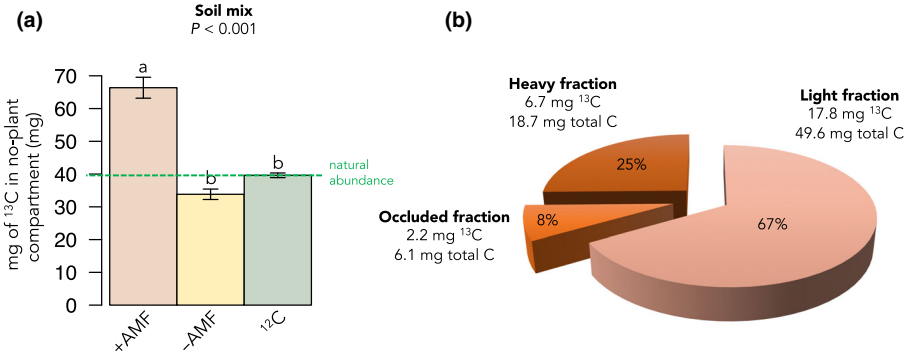


**Fig. 2** Total carbon (C) and $^{13}C$ transported by the arbuscular mycorrhizal fungus (AMF) *Rhizophagus intraradices* into a no-plant compartment and separated by soil organic matter fractions. (a) mg $^{13}C$ in soil mix (no-plant compartment) in AMF-permitted $^{13}C$ microcosms ('+AMF'), AMF-excluded $^{13}C$ microcosms ('−AMF'), and AMF-permitted $^{12}C$ microcosms ('$^{12}C$') after 6 wk of $^{13}CO_2$ labeling of host plant *Avena barbata*. Different letters above bars represent statistically significant differences (one-way ANOVA and Fisher's LSD test); corresponding *P*-value is indicated above the plot. Error bars represent SE ($n = 24$). The dashed green line represents the natural abundance level of $^{13}C$. (b) Distribution of $^{13}C$ contributed by AMF hyphae in light, occluded, and heavy soil fractions after 6 wk of labeling based on soil density fractionation followed by $^{13}C$ isotope ratio mass spectrometry (IRMS) analysis.



© 2024 The Authors
*New Phytologist* © 2024 New Phytologist Foundation

14698137, 0, Downloaded from https://nph.onlinelibrary.wiley.com/doi/10.1111/nph.19560, Wiley Online Library on [03/04/2024]. See the Terms and Conditions (https://onlinelibrary.wiley.com/terms-and-conditions) on Wiley Online Library for rules of use; OA articles are governed by the applicable Creative Commons License

14698137, 0, Downloaded from https://nph.onlinelibrary.wiley.com/doi/10.1111/nph.19560, Wiley Online Library on [03/04/2024]. See the Terms and Conditions (https://onlinelibrary.wiley.com/terms-and-conditions) on Wiley Online Library for rules of use; OA articles are governed by the applicable Creative Commons License

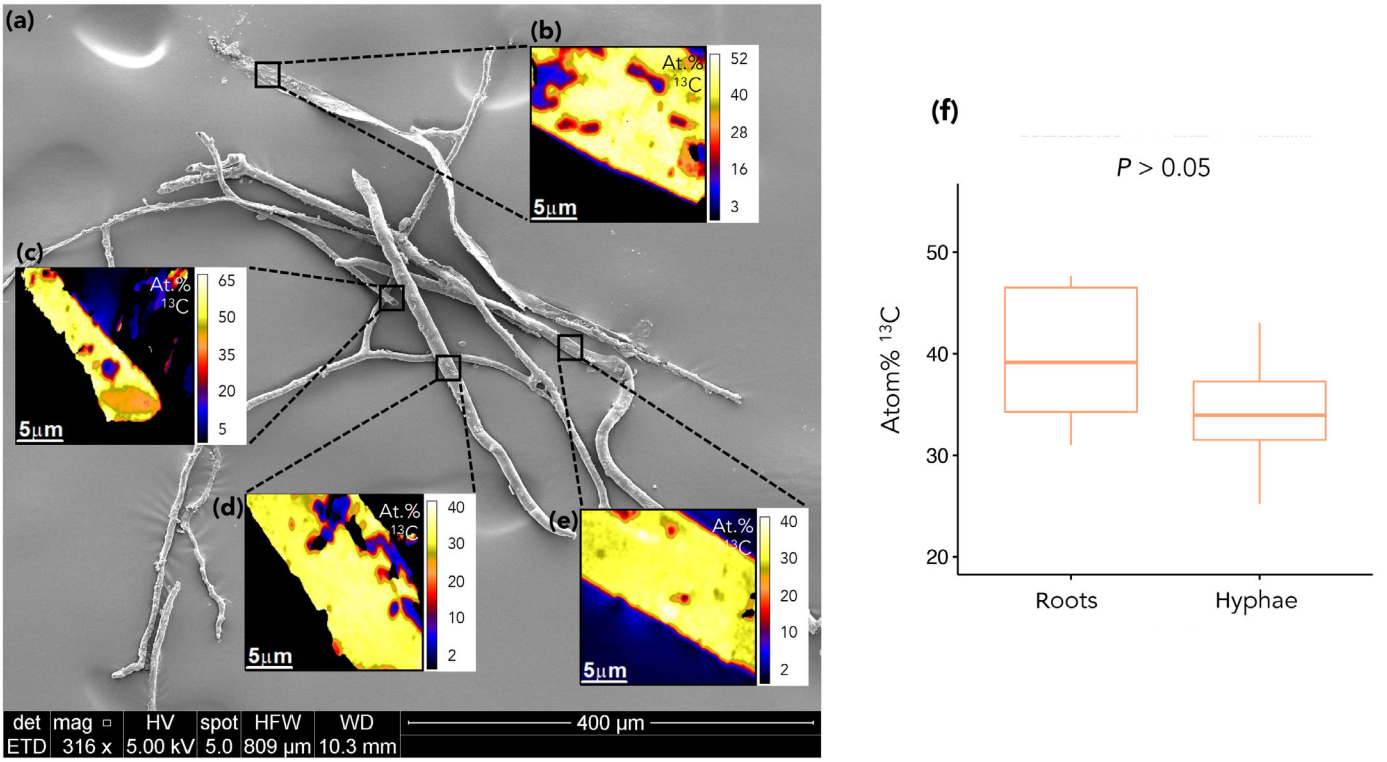


**Fig. 3** $^{13}C$ isotope enrichment of roots of the host plant *Avena barbata* and hyphae of the arbuscular mycorrhizal fungus (AMF) *Rhizophagus intraradices*. (a) Scanning electron microscopy image and (b–e) nanoscale secondary ion mass spectrometry (NanoSIMS) $^{13}C$ abundance images of hyphae from the no-plant compartment of an AMF-permitted $^{13}C$ microcosm ('+AMF'). Areas with cooler colors (black, blue) have a lower atom% $^{13}C$ while areas with warmer colors (orange, yellow) have a higher atom% $^{13}C$. (f) Atom% $^{13}C$ of roots and hyphae from +AMF microcosms. Atom% $^{13}C$ of roots was measured by isotope ratio mass spectrometry (IRMS). Atom% $^{13}C$ of hyphae was calculated using the average of 37 NanoSIMS images. Whiskers represent the minimum and maximum values in the data; *P*-value is indicated above the plot (paired Wilcoxon test, $n = 5$).

Fig. 4). The NMR spectra for +AMF soil mix samples show greater variability and slightly higher peaks in the 45–110 ppm region, corresponding to the O-alkyl C functional group and indicative of carbohydrates (Kögel-Knabner, 1997), which is not observed anywhere else in the spectra (Fig. 4).

## Hyphosphere community changes in response to AMF

There were no significant differences in the number of 16S sequences obtained from +AMF (32 451 ± 4596) vs −AMF (34 171 ± 6655) treatments after quality control. The 12 samples analyzed resulted in 3019 amplicon sequencing variants (ASVs), with 23 502–41 551 sequences per sample. There was no significant difference in the alpha diversity of prokaryotic communities in +AMF vs −AMF microcosms, as measured by richness, Shannon index, evenness, and Faith's phylogenetic diversity (ANOVA, $P > 0.05$). However, community composition did differ between +AMF and −AMF treatments (Fig. 5a), measured via permutational multivariate analysis of variance (Adonis, $F_{1,8} = 2.23$, $P = 0.004$).

DESEQ analysis identified 19 ASVs that were significantly more abundant in the presence of AMF, and 17 ASVs that were

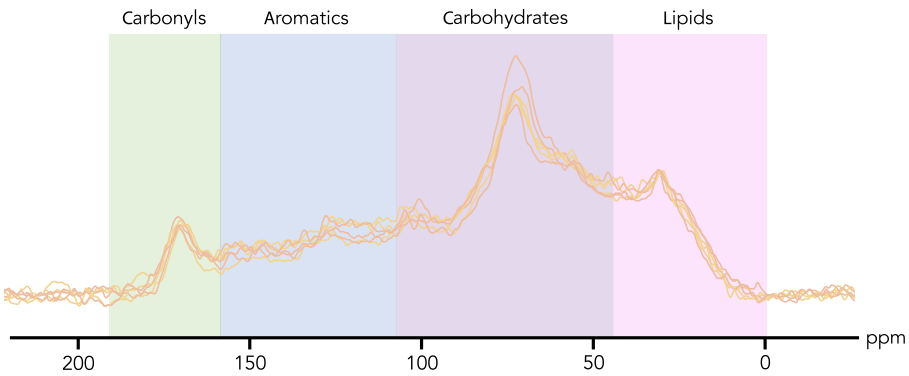


**Fig. 4** Solid-state $^{13}C$ nuclear magnetic resonance (NMR) spectra of the soil mix (no-plant compartment) of six microcosms. Three soil mix samples were from compartments accessible to hyphae of the arbuscular mycorrhizal fungus (AMF) *Rhizophagus intraradices* ('+AMF', in orange). Three soil mix samples were from compartments inaccessible to AMF hyphae ('−AMF', in yellow). Spectra intensities were normalized to the resonance at *ca.* 30 ppm.

© 2024 The Authors
*New Phytologist* © 2024 New Phytologist Foundation

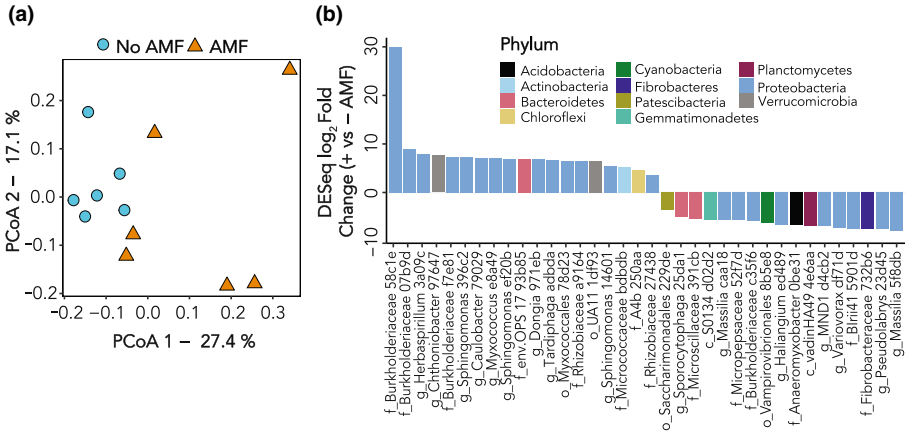


**Fig. 5** Bacterial community composition in the soil mix (no-plant compartment) of 12 microcosms based on 16S rRNA gene amplicons. Six soil mix samples were from compartments accessible to hyphae of the arbuscular mycorrhizal fungus (AMF) *Rhizophagus intraradices* ('+AMF'). Six soil mix samples were from compartments inaccessible to AMF hyphae ('−AMF'). (a) Principal component analysis showing distinct community composition with or without AMF. (b) Amplicon sequence variants that significantly increased and decreased in relative abundance in +AMF microcosms compared to −AMF microcosms (DESEQ analysis of 16S rRNA reads, $P < 0.05$ adjusted for multiple comparisons).

significantly less abundant in the presence of AMF (Fig. 5b; Table S4). Twenty-three of these 36 (65%) ASVs belong to the Proteobacteria Phylum. Fourteen increased in relative abundance in +AMF microcosms, and nine decreased. Other ASVs that significantly increased or decreased in relative abundance in +AMF microcosms are listed in Table S4.

### $^{13}$C enrichment of hyphosphere bacteria

Of the 3019 ASVs detected by 16S amplicon analysis, 2934 ASVs also had a semiperfect read match within the SIP-metagenomics dataset. We identified 92 ASVs significantly enriched in $^{13}$C (Fig. 6) among the total 682 ASVs that passed the QSIP criteria (e.g. detected in enough replicates and fractions). These ASVs span a diverse phylogeny, with Proteobacteria the dominant phylum. The most enriched taxa, with atom percent excess (APE) $^{13}C > 20\%$, include those from the delta-Proteobacteria order Myxococcales, Thaumarchaeota family Nitrososphaeraceae, the Acidobacteria genus Candidatus *Solibacter*, and the Bacteroidetes family AKYH767 (within the Sphingobacteriales). The most enriched ASV was from the *Haliangium* genus within the Myxococcales (APE 35.2%), an enrichment value similar to the AMF hyphae (35.9%) (note, Myxococcales has been proposed to be reorganized as the Myxococcota phylum in the GTDB taxonomy; Parks *et al.*, 2018). There were 33 ASVs from diverse phylum and orders with APE of over 10% (Fig. 6).

## Discussion

Arbuscular mycorrhizal fungi transport a significant amount of photosynthetic C into the soil matrix beyond the extent of roots alone, but the contribution of AMF to soil C retention lacks experimental exploration. We used $^{13}CO_2$ labeling of *A. barbata* in a two-compartment microcosm with an air gap designed to isolate *R. intraradices* hyphae from roots and quantify the amount and form of photosynthetic C transported via AMF hyphae into soil. After 6 wk of labeling, AMF hyphae crossing the air gap were $^{13}$C enriched at over 35 atom% and the total C transferred by hyphae and retained in soil represented over 2% of the total soil C, a third of which was found occluded within soil aggregates or stabilized in the mineral-associated fraction.

### AMF-transported C quickly enters protected pools

After 6 wk of labeling, the $^{13}$C that remained within the no-plant compartment soil included $^{13}$C that was fixed by plants, transferred to AMF, and transported to the no-plant compartment, minus the $^{13}$C that left the system via soil respiration or dissolved organic carbon (DOC) in water that drained from the microcosms. Thirty-three percent of this remaining $^{13}$C was in either the occluded fraction or the heavy fraction. Organic C in both fractions is thought to be at least somewhat protected from decomposition by its location inside aggregates or its association with minerals (Kleber *et al.*, 2007; Keiluweit *et al.*, 2012; Throckmorton *et al.*, 2015; Kallenbach *et al.*, 2016).

The $^{13}$C enrichment of soil density fractions suggests that a large portion of the AMF-derived C was still present in the form of living or dead hyphae, with 67% of the $^{13}$C in the light fraction. The density of a fungal hypha has been estimated to be 1.1 g cm$^{-3}$ (Bakken & Olsen, 1983), so hyphae should be concentrated in the light fraction unless they are in a protected form. Organic C in the light fraction is readily available to microbial and physical degradation and therefore tends to have a shorter residence time in soil compared with C in occluded and heavy fractions (Kleber *et al.*, 2007; Keiluweit *et al.*, 2012; Throckmorton *et al.*, 2015; Kallenbach *et al.*, 2016).

We found that a small fraction of the $^{13}$C, 8%, was in the occluded fraction inside aggregates that were sufficiently stable to retain structure and hold on to the $^{13}$C during the soil density fractionation process. As soil aggregation can physically protect C-rich litter from microbial degradation, an increase in aggregation may be an important mechanism for C sequestration (Rillig, 2004; Rillig & Mummey, 2006; Rillig *et al.*, 2010). Arbuscular mycorrhizal fungi may increase the stability of soil aggregates by producing and releasing glomalin-related soil glycoproteins (GRSP) (Wright *et al.*, 1996; Rillig *et al.*, 2001a,b, 2002, 2010; Halvorson & Gonzalez, 2006). A recent review, however, argues that the evidence supporting the production of GRSP by AMF is primarily correlative and GRSP may have multiple non-AMF origins (Holátko *et al.*, 2020). It is clear that AMF hyphae can increase soil aggregation by physically holding soil particles together in their intricate extraradical mycelium.



© 2024 The Authors
*New Phytologist* © 2024 New Phytologist Foundation

14698137, 0, Downloaded from https://nph.onlinelibrary.wiley.com/doi/10.1111/nph.19560, Wiley Online Library on [03/04/2024]. See the Terms and Conditions (https://onlinelibrary.wiley.com/terms-and-conditions) on Wiley Online Library for rules of use; OA articles are governed by the applicable Creative Commons License

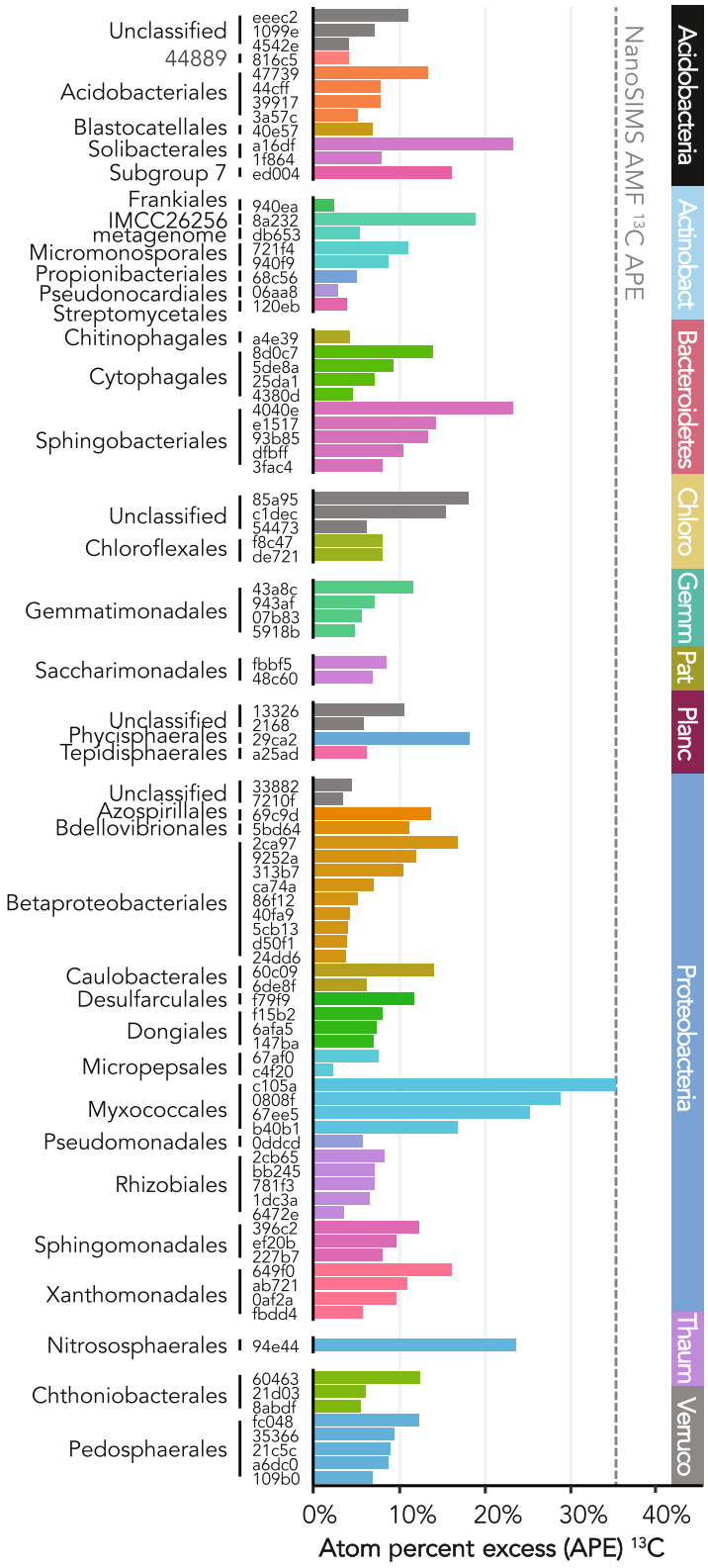


**Fig. 6** Following DNA-Stable Isotope Probing (DNA-SIP), $^{13}$C-enriched hyphosphere taxa and their level of enrichment in $^{13}$C atom% excess (APE). The amplicon sequence variants (ASVs, first five alphanumeric characters shown) are SIP-metagenomic reads that were mapped to corresponding ASVs obtained from 16S amplicon sequencing of the same DNA samples. Bars are grouped by Phylum of the ASVs and colored by Order. The dashed line shows the APE of hyphae of the arbuscular mycorrhizal fungus (AMF) *Rhizophagus intraradices* estimated by nanoscale secondary ion mass spectrometry (NanoSIMS).

© 2024 The Authors
*New Phytologist* © 2024 New Phytologist Foundation



14698137, 0, Downloaded from https://nph.onlinelibrary.wiley.com/doi/10.1111/nph.19560, Wiley Online Library on [03/04/2024]. See the Terms and Conditions (https://onlinelibrary.wiley.com/terms-and-conditions) on Wiley Online Library for rules of use; OA articles are governed by the applicable Creative Commons License

The physical protection of C in aggregates can be visually observed in Fig. 1(d) where soil aggregates were mechanically broken open to reveal AMF hyphae.

Lastly, *c.* 25% of the transported $^{13}C$ remained in soil within the heavy fraction. The origin of this mineral-associated organic C may have been hyphal exudates, hyphae that senesced and degraded to the point of being sorbed to mineral surfaces, or bacteria that consumed the exudates or hyphae (Pett-Ridge & Firestone, 2017). The transfer of root C into fungal and bacterial cell biomass appears to be a particularly important step that precedes C stabilization on mineral surfaces (Kleber *et al.*, 2007, 2015; Keiluweit *et al.*, 2012; Cotrufo *et al.*, 2013: Throckmorton *et al.*, 2015; Kallenbach *et al.*, 2016; Pett-Ridge & Firestone, 2017). In an earlier glasshouse study, we used soil collected from the same field site and the same plant genus, but used only one compartment for both roots and hyphae. We found 43% of the C from root and hyphae in the heavy fraction after 12 wk of labeling (Pett-Ridge & Firestone, 2017). Carbon contributed by hyphae alone was more than half of that from both roots and hyphae, despite the shorter labeling time reported here (6 wk) compared to that of the previous study. Both sets of results demonstrate rapid interactions between root and hyphal exudates and soil minerals.

## AMF contribute significant soil C

In our experiment, C transported by AMF hyphae made up over 2% of the total organic C in the no-plant compartment after a 6-wk incubation. This amount of organic C is substantial relative to the estimate that up to 5% of the total organic C in soil is from living microbial biomass (Paul & Clark, 1989). This comparison is necessarily approximate because we do not know the effects that the no-plant compartment characteristics (1 : 1 mix of soil and sand, an air gap, and only 6 wk to develop) may have had relative to natural soil under equilibrium conditions. Nonetheless, this finding is consistent with estimates that AMF are 15–30% of the total soil microbial biomass in natural soil (Olsson & Wilhelmsson, 2000; Rillig *et al.*, 2001b; Leake *et al.*, 2004; Qin *et al.*, 2017). Arbuscular mycorrhizal fungi have been observed to spread over 11 cm away from roots in a pot culture in 7 wk (Jakobsen *et al.*, 1992), which is in line with observations in our study. It appears that AMF have the ability to grow hyphal networks quickly and thus rapidly distribute a substantial amount of C into the soil.

Notably, we did not measure DOC in the hyphal compartment. As such, our calculations do not take into account any $^{13}C$ that desorbed into the supernatant during the fractionation process, or $^{13}C$ that left the system via water that drained from the microcosms. Root and hyphal exudates in the form of DOC are key substrates for soil microbes and part of the pathway that generates mineral-associated forms of soil C, suggesting that our results may be an underestimation of the contribution of AMF to soil C pools.

In the NMR spectra, the presence of AMF seems to impact the 45–110 ppm region, typically associated with O-alkyl C, or carbohydrates, more than any other regions (Fig. 4). A higher peak in this region would be consistent with an increase in carbohydrate-rich biomass or hyphal deposition. While the −AMF soils all have a similar peak height and shape in this spectral region, some of the +AMF replicates have a broader or higher peak. It was not possible to standardize the amount of hyphal biomass or hyphal exudate in the soil samples from the no-plant compartments analyzed by NMR, but it seems probable that at least one of the +AMF samples had a greater amount of a carbohydrate-like compound, leading to a higher peak. This would suggest that AMF in the soil away from the direct influence of roots produced hyphae and/or released metabolites that contained a large proportion of carbohydrates. Arbuscular mycorrhizal fungi hyphae contain structural chitin (an aminopolysaccharide) and are known to exude diverse compounds in the hyphosphere, including sugars (in particular hexoses) (Toljander *et al.*, 2007; Bharadwaj *et al.*, 2012; Sato *et al.*, 2015; Luthfiana *et al.*, 2021), so our observations of increased hyphosphere carbohydrates appear consistent with previous studies.

## Enrichment of AMF C is comparable to that of roots

The NanoSIMS results show there was no significant difference between the $^{13}C$ enrichment of roots and hyphae (Fig. 3f). Hyphae have been shown not only to bring plants nutrients but also to carry up to 34% of the water transpired by plants (Ruth *et al.*, 2011; Quiroga *et al.*, 2019; Kakouridis *et al.*, 2022). In fact, the evolution of land plants may have only been possible through the formation of mycorrhizal associations, because the algal ancestors to land plants were not adequately equipped to live on land independently (Jeffrey, 1962; Pirozynski & Malloch, 1975; van der Heijden *et al.*, 2015). NanoSIMS evidence from this study further supports the idea that AMF truly act as an extension of the root system.

## Composition and activity of AMF hyphosphere microbial communities

Local-scale soil biogeochemistry is an important driver of microbial community composition (McGuire & Treseder, 2010; Wagg *et al.*, 2014; Graham *et al.*, 2016; Anthony *et al.*, 2020; Kivlin *et al.*, 2020). We were interested in how AMF affect the soil microbial community – separately from roots – which we assessed with both $^{13}C$-SIP analysis and amplicon 16S sequencing. These two methods ask fundamentally different questions: $^{13}C$-SIP asks what organisms partake in the AMF-C food web, either peripherally (low $^{13}C$ enrichment) or centrally (high $^{13}C$ enrichment), while amplicon sequencing asks how the presence vs absence of AMF enables dramatic (e.g. $\log_2$fold) changes in the relative abundance of taxa. These two methods provide critical but different perspectives on the composition and activity of hyphosphere microbial communities.

Arbuscular mycorrhizal fungi frequently co-occur with bacteria in soil away from the direct influence of roots (Yuan *et al.*, 2021). Here, using 16S amplicon analysis, we found that the relative abundance of 19 ASVs significantly increased and the



© 2024 The Authors
*New Phytologist* © 2024 New Phytologist Foundation

14698137, 0, Downloaded from https://nph.onlinelibrary.wiley.com/doi/10.1111/nph.19560, Wiley Online Library on [03/04/2024]. See the Terms and Conditions (https://onlinelibrary.wiley.com/terms-and-conditions) on Wiley Online Library for rules of use; OA articles are governed by the applicable Creative Commons License

relative abundance of 17 ASVs significantly decreased in the presence of AMF in the root-free hyphal compartment. Over half of these changed ASVs belonged to the Proteobacteria Phylum, suggesting a potential phylogenetic coherence of bacteria whose abundances strongly respond to the presence of AMF. These 36 ASVs only comprise 1.2% of all ASVs detected, but their abundance changes were sufficiently large to shift the overall community structure, as other studies have also discovered (Nuccio *et al.*, 2013; Gui *et al.*, 2017; Rodríguez-Caballero *et al.*, 2017; Cao *et al.*, 2020; Hao *et al.*, 2020).

Some of the taxa that increased in abundance did not incorporate $^{13}$C. Two ASVs of the Burkholderiaceae family (58c1e and 07b9d) increased the most in relative abundance among all ASVs but were not $^{13}$C enriched. Arbuscular mycorrhizal fungi may have stimulated these organisms by mechanisms that did not involve $^{13}$C consumption, such as by changing local edaphic or nutrient conditions (e.g. increasing or decreasing N, P) or by non-assimilative C processes. In addition, we were unable to determine whether 10 of the 19 ASVs that increased in relative abundance incorporated $^{13}$C.

Compared with amplicon analysis, $^{13}$C-SIP identified many more organisms in the AMF food web. DNA-SIP isolates the populations actively assimilating a labeled substrate and does not detect DNA from inactive microbes, relic DNA fragments, or slow-growing communities. Even though only 23% of the ASVs detected via amplicon sequencing were captured by metagenomics and subsequent QSIP analysis, QSIP detected many organisms that took up $^{13}$C without detectable changes in relative abundance. The AMF hyphosphere is a microhabitat that can be difficult to isolate and sample without also collecting large amounts of background soil; in these instances, SIP may more sensitively identify populations responding to AMF than standard amplicon analyses. However, since shotgun metagenomic sequencing can hardly capture all 16S genes from a soil community, the true AMF food web likely contains more taxa than detected in this study.

This study goes beyond our previous work (Nuccio *et al.*, 2022) by using 16S amplicon sequences from the same DNA samples as a reference database to identify more $^{13}$C-enriched hyphosphere taxa within our SIP-metagenomes. Previously, we used metagenome assembled genomes (MAGs), which limits the analysis to genomes amenable to assembly. In line with our previous findings, the three most enriched ASVs, including one with $^{13}$C enrichment close to that of AMF hyphae, all belong to the family Myxococcales in the genus Haliangium, likely facultative predators (Nuccio *et al.*, 2022). An ammonia-oxidizing archaea (AOA), Nitrososphaera, was also highly enriched with 23% APE. We also identified multiple highly $^{13}$C enriched taxa that were not assembled into MAGs in our previous study. For example, ASVs belonging to Solibacterales, Subgroup 7, and Phycisphaerales were $^{13}$C enriched with over or nearly 20% APE. Solibacterales taxa are known to solubilize phosphorous (Bergkemper *et al.*, 2016), which may synergistically interact with AMF by P-C exchange (Nacoon *et al.*, 2020). Acidobacteria Subgroup 7 is reported to increase with pH (Jones *et al.*, 2009) and has potential to use different carbohydrates (de Chaves *et al.*, 2019). The high $^{13}$C enrichment of this Acidobacteria subgroup may be a combination of microhabitat change and substrate availability associated with AMF but needs further study. The Phycisphaerales ASV matched well to soil microbes from other studies (Zeglin *et al.*, 2016; Addison *et al.*, 2019), and our finding that it consumed AMF-derived C may be a first clue about its function in soil.

Some ASVs with moderate APE that are from Orders Rhizobiales, Caulobacterales, Sphingomonadales have been reported to associate with AMF (Hoseinzade *et al.*, 2016; Agnolucci *et al.*, 2019; Akyol *et al.*, 2019; Hao *et al.*, 2020; Yuan *et al.*, 2021). Here, we confirmed their consumption of hyphae-derived C. Rhizobiales and Sphingomonadales are considered rhizosphere adaptors (Lei *et al.*, 2019) and together consist of 4.8% of the total AMF hyphosphere ASVs in our study. The hyphosphere may have similar characteristics to the rhizosphere, in that low-molecular-weight C from hyphal exudates selectively enriches these taxa. Their moderate but not high levels of $^{13}$C incorporation may be limited by the relatively small portion of the cells that are spatially close to hyphae and have access to AMF C. The photosynthetic C transported by AMF thus facilitated a diverse hyphosphere microbial food web dependent on AMF hyphal C supply.

Taxa in the hyphosphere food web may contribute to incorporating AMF-derived C into soil, SOM formation, and stabilization. Resources derived from hyphae can increase microbial biomass, activity, frequency of interactions, and the rate of organic matter transformations (Sokol *et al.*, 2022). Necromass from these microbial cells is also likely a significant source of SOM and may have formed part of the mineral-associated C that we recovered from the soil heavy fraction (Fossum *et al.*, 2022; Sokol *et al.*, 2022; Hu *et al.*, 2023). Future studies that compare the AMF hyphosphere with and without its microbiome would be needed to quantify this contribution.

## Conclusion

Our study shows that AMF move a substantial amount of C from plants beyond the rhizosphere. After only a few weeks, about a third of this mobilized C had made its way into aggregate-occluded and mineral-associated forms, which may have longer residence times in soil. In hyphosphere soil, we measured an increased presence of organic C compounds (such as chitin and hexoses) that are generally associated with AMF hyphae. Arbuscular mycorrhizal fungi C inputs modified the hyphosphere bacterial community, facilitating a diverse microbial food web that incorporated hyphae-derived C. This effect likely stimulated enhanced AMF (and thereby plant) access to N and P. Together, our findings indicate that AMF play a key role in the formation of SOM and thus could be employed in strategies for climate change mitigation and sustainable land management.

## Acknowledgements

The authors thank Dr Thomas D. Bruns and Dr John W. Taylor for their thoughtful advice on the project, Donald J. Herman

© 2024 The Authors
*New Phytologist* © 2024 New Phytologist Foundation



14698137, 0, Downloaded from https://nph.onlinelibrary.wiley.com/doi/10.1111/nph.19560, Wiley Online Library on [03/04/2024]. See the Terms and Conditions (https://onlinelibrary.wiley.com/terms-and-conditions) on Wiley Online Library for rules of use; OA articles are governed by the applicable Creative Commons License

and Christina M. Wistrom for their assistance with the glasshouse setup, Dr Denise Schichnes and Dr Steven E. Ruzin for their guidance with microscopy, Christina E. Ramon for her assistance with sample preparation for SEM and NanoSims, and Dr Michael S. Page for his help with $^{13}C$ calculations and support with final edits. This research was supported by the US Department of Energy Office of Science, Office of Biological and Environmental Research Genomic Science program under Awards DE-SC0016247 and DE-SC0020163 to UC Berkeley and Awards SCW1589 and SCW1678 to Lawrence Livermore National Laboratory. Work conducted at LLNL was performed under the auspices of the US Department of Energy under Contract DE-AC52-07NA27344. AK was supported by the Bennett Agricultural Fellowship, the Storie Memorial Fellowship, and the Jenny Fellowship in Soil Science.

## Competing interests

None declared.

## Author contributions

AK and MKF designed the experiment with the assistance of JAH, MY, KYE-M, EEN and JP-R. AK, JAH, MLM, CAF, and PKW performed the experiment with assistance from KYE-M. AK, JAH, MY, EEN, CAF, MLM, PSN, PKW and MKF analyzed the data with the assistance of KYE-M and JP-R. AK, MY, EEN, JP-R and MKF drafted the manuscript. AK, MY, EEN, JAH, CAF, KYE-M, PSN, PKW, JP-R and MKF all contributed to the final manuscript.

## ORCID

Katerina Y. Estera-Molina https://orcid.org/0000-0001-5217-8757
Mary K. Firestone https://orcid.org/0000-0002-4289-3244
Christina A. Fossum https://orcid.org/0000-0002-6499-357X
John A. Hagen https://orcid.org/0000-0002-7396-9707
Anne Kakouridis https://orcid.org/0000-0003-1627-3444
Madeline L. Moore https://orcid.org/0000-0002-4864-6527
Peter S. Nico https://orcid.org/0000-0002-4180-9397
Erin E. Nuccio https://orcid.org/0000-0003-0189-183X
Jennifer Pett-Ridge https://orcid.org/0000-0002-4439-2398
Peter K. Weber https://orcid.org/0000-0001-6022-6050
Mengting Yuan https://orcid.org/0000-0003-0017-3908

## Data availability

The data that support the findings of this study are openly available in the main text, supporting information, and stored in SRA under project ID PRJNA1051335.

## References

**Addison S, Smaill S, Garrett L, Wakelin S. 2019.** Effects of forest harvest and fertiliser amendment on soil biodiversity and function can persist for decades. *Soil Biology and Biochemistry* **135**: 194–205.

**Agnolucci M, Avio L, Pepe A, Turrini A, Cristani C, Bonini P, Cirino V, Colosimo F, Ruzzi M, Giovannetti M. 2019.** Bacteria associated with a commercial mycorrhizal inoculum: community composition and multifunctional activity as assessed by Illumina sequencing and culture-dependent tools. *Frontiers in Plant Science* **9**: 1956.

**Akyol TY, Niwa R, Hirakawa H, Maruyama H, Sato T, Suzuki T, Fukunaga A, Sato T, Yoshida S, Tawaraya K *et al.* 2019.** Impact of introduction of arbuscular mycorrhizal fungi on the root microbial community in agricultural fields. *Microbes and Environments* **34**: 23–32.

**Angst G, Mueller KE, Nierop KG, Simpson MJ. 2021.** Plant- or microbial-derived? A review on the molecular composition of stabilized soil organic matter. *Soil Biology and Biochemistry* **156**: 108–189.

**Anthony MA, Crowther TW, Maynard DS, van den Hoogen J, Averill C. 2020.** Distinct assembly processes and microbial communities constrain soil organic carbon formation. *One Earth* **2**: 349–360.

**Bakken LR, Olsen RA. 1983.** Buoyant densities and dry-matter contents of microorganisms: conversion of a measured biovolume into biomass. *Applied and Environmental Microbiology* **45**: 1188–1195.

**Bergkemper F, Kublik S, Lang F, Krüger J, Vestergaard G, Schloter M, Schulz S. 2016.** Novel oligonucleotide primers reveal a high diversity of microbes which drive phosphorous turnover in soil. *Journal of Microbiological Methods* **125**: 91–97.

**Bharadwaj DP, Alström S, Lundquist P. 2012.** Interactions among *Glomus irregulare*, arbuscular mycorrhizal spore-associated bacteria, and plant pathogens under *in vitro* conditions. *Mycorrhiza* **22**: 437–447.

**Bolyen E, Rideout JR, Dillon MR, Bokuich NA, Abnet CC, Al-Ghalith A, Alexander H, Alm EJ, Arumugam M, Asnicar F *et al.* 2019.** Reproducible, interactive, scalable and extensible microbiome data science using QIIME 2. *Nature Biotechnology* **37**: 852–857.

**Brodie EL, Joyner DC, Faybishenko B, Conrad ME, Rios-Velazquez C, Malave J, Martinez R, Mork B, Willett A, Koenigsberg S *et al.* 2011.** Microbial community response to addition of polylactate compounds to stimulate hexavalent chromium reduction in groundwater. *Chemosphere* **85**: 660–665.

**Bunn RA, Simpson DT, Bullington LS, Leckberg Y, Janos DP. 2019.** Revisiting the 'direct mineral cycling' hypothesis: arbuscular mycorrhizal fungi colonize leaf litter, but why? *The ISME Journal* **13**: 1891–1898.

**Bushnell B. 2014.** *BBTOOLS software package.* [WWW document] URL sourceforge.net/projects/bbmap/ [accessed 2 April 2022].

**Callahan BJ, McMurdie PJ, Rosen MJ, Han AW, Johnson AJ, Holmes SP. 2016.** DADA2: high-resolution sample inference from Illumina amplicon data. *Nature Methods* **13**: 581–583.

**Cao J, Feng Y, Lin X, Wang J. 2020.** A beneficial role of arbuscular mycorrhizal fungi in influencing the effects of silver nanoparticles on plant-microbe systems in a soil matrix. *Environmental Science and Pollution Research* **27**: 11782–11796.

**Caporaso JG, Lauber CL, Walters WA, Berg-Lyons D, Huntley J, Fierer N, Owens M, Betley J, Fraser L, Bauer M *et al.* 2012.** Ultra-high-throughput microbial community analysis on the Illumina HiSeq and MiSeq platforms. *The ISME Journal* **6**: 1621–1624.

**de Chaves M, Silva G, Rossetto R, Edwards R, Tsai S, Navarrete A. 2019.** Acidobacteria subgroups and their metabolic potential for carbon degradation in sugarcane soil amended with vinasse and nitrogen fertilizers. *Frontiers in Microbiology* **10**: 467603.

**Cheeke TE, Phillips RP, Brzostek ER, Rosling A, Bever JD, Fransson P. 2016.** Dominant mycorrhizal association of trees alters carbon and nutrient cycling by selecting for microbial groups with distinct enzyme function. *New Phytologist* **214**: 432–442.

**Cheng L, Booker FL, Tu C, Burkey KO, Zhou L, Shew HD, Rufty TW, Hu S. 2012.** Arbuscular mycorrhizal fungi increase organic carbon decomposition under elevated $CO_2$. *Science* **337**: 1084–1087.

**Cotrufo MF, Wallenstein MD, Boot CM, Denef K, Paul E. 2013.** The microbial efficiency-matrix stabilization (MEMS) framework integrates plant litter decomposition with soil organic matter stabilization: do labile plant inputs form stable soil organic matter? *Global Change Biology* **19**: 988–995.

**Domeignoz-Horta LA, Shinfuku M, Junier P, Poirier S, Verrecchia E, Sebag D, DeAngelis KM. 2021.** Direct evidence for the role of microbial community



© 2024 The Authors
*New Phytologist* © 2024 New Phytologist Foundation

14698137, 0, Downloaded from https://nph.onlinelibrary.wiley.com/doi/10.1111/nph.19560, Wiley Online Library on [03/04/2024]. See the Terms and Conditions (https://onlinelibrary.wiley.com/terms-and-conditions) on Wiley Online Library for rules of use; OA articles are governed by the applicable Creative Commons License

composition in the formation of soil organic matter composition and persistence. *ISME Communications* **1**: 64.

**Dumbrell AJ, Ashton PD, Aziz N, Feng G, Nelson M, Dytham C, Fitter AH, Helgason T. 2011.** Distinct seasonal assemblages of arbuscular mycorrhizal fungi revealed by massively parallel pyrosequencing. *New Phytologist* **190**: 794–804.

**Dynarski KA, Bossio DA, Scow KM. 2020.** Dynamic stability of soil carbon: reassessing the "permanence" of soil carbon sequestration. *Frontiers in Environmental Science* **8**: 514701.

**Fossum C, Estera-Molina KY, Yuan M, Herman DJ, Chu-Jacoby I, Nico PS, Morrison KD, Pett-Ridge J, Firestone MK. 2022.** Belowground allocation and dynamics of recently fixed plant carbon in a California annual grassland. *Soil Biology and Biochemistry* **165**: 108519.

**Frey SD. 2019.** Mycorrhizal fungi as mediators of soil organic matter dynamics. *Annual Review of Ecology, Evolution, and Systematics* **50**: 237–259.

**Ghosal S, Fallon SJ, Leighton TJ, Wheeler KE, Kristo MJ, Hutcheon ID, Weber PK. 2008.** Imaging and 3D elemental characterization of intact bacterial spores by high-resolution secondary ion mass spectrometry. *Analytical Chemistry* **80**: 5986–5992.

**Godbold DL, Hoosbeek MR, Lukac M, Cotrufo MF, Janssens IA, Ceulemans R, Polle A, Velthorst EJ, Scarascia-Mugnozza G, De Angelis P *et al.* 2006.** Mycorrhizal hyphal turnover as a dominant process for carbon input into soil organic matter. *Plant and Soil* **281**: 15–24.

**Graham EB, Knelman JE, Schindlbacher A, Siciliano S, Breulmann M, Yannarell A, Beman JM, Abell G, Philippot L, Prosser J *et al.* 2016.** Microbes as engines of ecosystem function: when does community structure enhance predictions of ecosystem processes? *Frontiers in Microbiology* **7**: 1–10.

**Gui H, Purahong W, Hyde KD, Xu J, Mortimer PE. 2017.** The arbuscular mycorrhizal fungus *Funneliformis mosseae* alters bacterial communities in subtropical forest soils during litter decomposition. *Frontiers in Microbiology* **8**: 1120.

**Habte M, Osorio NW. 2001.** *Arbuscular mycorrhizas: producing and applying arbuscular mycorrhizal inoculum.* Honolulu, HI, USA: College of Tropical Agriculture and Human Resources, University of Hawai'i, Manoa.

**Halvorson JJ, Gonzalez JM. 2006.** Bradford reactive soil protein in Appalachian soils: distribution and response to incubation, extraction reagent and tannins. *Plant and Soil* **286**: 339–356.

**Hao X, Zhu YG, Nybroe O, Nicolaisen MH. 2020.** The composition and phosphorus cycling potential of bacterial communities associated with hyphae of *Penicillium* in soil are strongly affected by soil origin. *Frontiers in Microbiology* **10**: 2951.

**Hatton P-J, Kleber M, Zeller B, Moni C, Plante AF, Townsend K, Gelhaye L, Lajtha K, Derrien D. 2012.** Transfer of litter-derived N to soil mineral–organic associations: evidence from decadal $^{15}$N tracer experiments. *Organic Geochemistry* **42**: 1489–1501.

**Hawkins HJ, Cargill RI, Van Nuland ME, Hagen SC, Field KJ, Sheldrake M, Soudzilovskaia NA, Kiers ET. 2023.** Mycorrhizal mycelium as a global carbon pool. *Current Biology* **33**: R560–R573.

**Heckman K, Hicks Pries CE, Lawrence CR, Rasmussen C, Crow SE, Hoyt AM, von Fromm SF, Shi Z, Stoner S, McGrath C *et al.* 2022.** Beyond bulk: density fractions explain heterogeneity in global soil carbon abundance and persistence. *Global Change Biology* **28**: 1178–1196.

**van der Heijden MGA, Martin FM, Selosse M-A, Sanders IR. 2015.** Mycorrhizal ecology and evolution: the past, the present, and the future. *New Phytologist* **205**: 1406–1423.

**Herman DJ, Firestone MK, Nuccio E, Hodge A. 2012.** Interactions between an arbuscular mycorrhizal fungus and a soil microbial community mediating litter decomposition. *FEMS Microbiology Ecology* **80**: 236–247.

**Hestrin R, Kan M, Lafler M, Wollard J, Kimbrel JA, Ray P, Blazewicz S, Stuart R, Craven K, Firestone M *et al.* 2022.** Plant-associated fungi support bacterial resilience following water limitation. *The ISME Journal* **16**: 2752–2762.

**Hicks Pries CE, Sulman BN, West C, O'Neill C, Poppleton E, Porras RC, Castanha C, Zhu B, Wiedemeier DB, Torn MS. 2018.** Root litter decomposition slows with soil depth. *Soil Biology and Biochemistry* **125**: 103–114.

**Hodge A, Campbell C, Fitter A. 2001.** An arbuscular mycorrhizal fungus accelerates decomposition and acquires nitrogen directly from organic material. *Nature* **413**: 297–299.

**Holátko J, Brtnický M, Kučerík J, Kotianová M, Elbl J, Kintl A, Kynický J, Benada O, Datta R, Jansa J. 2020.** Glomalin – truths, myths, and the future of this elusive soil glycoprotein. *Soil Biology and Biochemistry* **153**: 108116.

**Hooker JE, Piatti P, Cheshire MV, Watson CA. 2007.** Polysaccharides and monosaccharides in the hyphosphere of the arbuscular mycorrhizal fungi *Glomus E3* and *Glomus tenue*. *Soil Biology and Biochemistry* **39**: 680–683.

**Horsch CCA, Antunes PM, Fahey C, Grandy AS, Kallenbach CM. 2023.** Trait-based assembly of arbuscular mycorrhizal fungal communities determines soil carbon formation and retention. *New Phytologist* **239**: 311–324.

**Hoseinzade H, Ardakani MR, Shahdi A, Asadi Rahmani H, Noormohammadi G, Miransari M. 2016.** Rice (*Oryza sativa* L.) nutrient management using mycorrhizal fungi and endophytic *Herbaspirillum seropedicae*. *Journal of Integrative Agriculture* **15**: 1385–1394.

**Hu J, Du M, Chen J, Tie L, Zhou S, Buckeridge KM, Cornelissen JHC, Huang C, Kuzyakov Y. 2023.** Microbial necromass under global change and implications for soil organic matter. *Global Change Biology* **29**: 3503–3515.

**Hungate BA, Mau RL, Schwartz E, Caporaso JG, Dijkstra P, van Gestel N, Koch BJ, Liu CM, McHugh TA, Marks JC *et al.* 2015.** Quantitative microbial ecology through stable isotope probing. *Applied and Environmental Microbiology* **81**: 7570–7581.

**Jakobsen I, Abbott LK, Robson AD. 1992.** External hyphae of vesicular-arbuscular mycorrhizal fungi associated with *Trifolium subterraneum* L. 1. Spread of hyphae and phosphorus inflow into roots. *New Phytologist* **120**: 371–380.

**Jakobsen I, Rosendahl L. 1990.** Carbon flow into soil and external hyphae from roots of mycorrhizal cucumber plants. *New Phytologist* **115**: 77–83.

**Jastrow JD, Amonette JE, Bailey VL. 2007.** Mechanisms controlling soil carbon turnover and their potential application for enhancing carbon sequestration. *Climate Change* **80**: 5–23.

**Jeffrey C. 1962.** The origin and differentiation of the Archegoniate land-plants. *Botaniska Notiser* **115**: 446–454.

**Jiang F, Zhang L, Zhou J, George TS, Feng G. 2021.** Arbuscular mycorrhizal fungi enhance mineralization of organic phosphorus by carrying bacteria along their extraradical hyphae. *New Phytologist* **230**: 304–315.

**Jones RT, Robeson MS, Lauber CL, Hamady M, Knight R, Fierer N. 2009.** A comprehensive survey of soil acidobacterial diversity using pyrosequencing and clone library analyses. *The ISME Journal* **3**: 442–453.

**Kaiser C, Kilburn MR, Clode PL, Fuchslueger L, Koranda M, Cliff JB, Solaiman ZM, Murphy DV. 2015.** Exploring the transfer of recent plant photosynthates to soil microbes: mycorrhizal pathway vs direct root exudation. *New Phytologist* **205**: 1537–1551.

**Kakouridis A. 2021.** *The role of arbuscular mycorrhizal fungi in ecosystems: water transport to plants, carbon transport to soil, and the assessment of drivers that shape their biodiversity.* PhD thesis, University of California, Berkeley, CA, USA.

**Kakouridis A, Hagen JA, Kan MP, Mambelli S, Feldman LJ, Herman DJ, Weber PK, Pett-Ridge J, Firestone MK. 2022.** Routes to roots: direct evidence of water transport by arbuscular mycorrhizal fungi to host plants. *New Phytologist* **236**: 210–221.

**Kallenbach CM, Frey SD, Grandy AS. 2016.** Direct evidence for microbial-derived soil organic matter formation and its ecophysiological controls. *Nature Communications* **7**: 13630.

**Keiluweit M, Bougoure JJ, Nico PS, Pett-Ridge J, Weber PK, Kleber M. 2015.** Mineral protection of soil carbon counteracted by root exudates. *Nature Climate Change* **5**: 588–595.

**Keiluweit M, Bougoure JJ, Zeglin LH, Myrold DD, Weber PK, Pett-Ridge J, Kleber M, Nico PS. 2012.** Nano-scale investigation of the association of microbial nitrogen residues with iron (hydr)oxides in a forest soil O-horizon. *Geochimica et Cosmochimica Acta* **95**: 213–226.

**Kembel SW, Cowan PD, Helmus MR, Cornwell WK, Morlon H, Ackerly DD, Blomberg SP, Webb CO. 2010.** PICANTE: R tools for integrating phylogenies and ecology. *Bioinformatics* **26**: 1463–1464.

**Kivlin SN, Fei S, Kalisz S, Averill C. 2020.** Microbial ecology meets macroecology: developing a process-based understanding of the microbial role in global ecosystems. *Bulletin of the Ecological Society of America* **101**: e01645.

**Kleber M, Eusterhues K, Keiluweit M, Mikutta C, Mikutta R, Nico P. 2015.** Mineral–organic associations: formation, properties, and relevance in soil environments. *Advances in Agronomy* **130**: 1–140.

© 2024 The Authors
*New Phytologist* © 2024 New Phytologist Foundation



14698137, 0, Downloaded from https://nph.onlinelibrary.wiley.com/doi/10.1111/nph.19560, Wiley Online Library on [03/04/2024]. See the Terms and Conditions (https://onlinelibrary.wiley.com/terms-and-conditions) on Wiley Online Library for rules of use; OA articles are governed by the applicable Creative Commons License

**Kleber M, Sollins P, Sutton R. 2007.** A conceptual model of organo-mineral interactions in soils: self-assembly of organic molecular fragments into zonal structures on mineral surfaces. *Biogeochemistry* **85**: 9–24.

**Koch BJ, McHugh TA, Hayer M, Schwartz E, Blazewicz SJ, Dijkstra P, van Gestel N, Marks JC, Mau RL, Morrissey EM *et al.* 2018.** Estimating taxon-specific population dynamics in intact microbial communities. *Ecosphere* **9**: e02090.

**Kögel-Knabner I. 1997.** $^{13}C$ and $^{15}N$ NMR spectroscopy as a tool in soil organic matter studies. *Geoderma* **80**: 243–270.

**Kögel-Knabner I. 2002.** The macromolecular organic composition of plant and microbial residues as inputs to soil organic matter. *Soil Biology and Biochemistry* **34**: 139–162.

**Lang AK, Jevon FV, Vietorisz CR, Ayres MP, Hatala Matthes J. 2021.** Fine roots and mycorrhizal fungi accelerate leaf litter decomposition in a northern hardwood forest regardless of dominant tree mycorrhizal associations. *New Phytologist* **230**: 316–326.

**Langley JA, Hungate BA. 2003.** Mycorrhizal controls on belowground litter quality. *Ecology* **84**: 2302–2312.

**Leake J, Johnson D, Donnelly D, Muckle G, Boddy L, Read D. 2004.** Networks of power and influence: the role of mycorrhizal mycelium in controlling plant communities and agroecosystem functioning. *Canadian Journal of Botany* **82**: 1016–1045.

**Lecomte J, St-Arnaud M, Hijri M. 2011.** Isolation and identification of soil bacteria growing at the expense of arbuscular mycorrhizal fungi. *FEMS Microbiology Letters* **317**: 43–51.

**Lee J, Lee S, Young PW. 2008.** Improved PCR primers for the detection and identification of arbuscular mycorrhizal fungi. *FEMS Microbiology Ecology* **65**: 339–349.

**Lehmann J, Hansel CM, Kaiser C, Kleber M, Maher K, Manzoni S, Nunan N, Reichstein M, Schimel JP, Manzoni S *et al.* 2020.** Persistence of soil organic carbon caused by functional complexity. *Nature Geoscience* **13**: 529–534.

**Lei S, Xu X, Cheng Z, Xiong J, Ma R, Zhang L, Yang X, Zhu Y, Zhang B, Tian B. 2019.** Analysis of the community composition and bacterial diversity of the rhizosphere microbiome across different plant taxa. *MicrobiologyOpen* **8**(6): e00762.

**Leifheit E, Verbruggen E, Rillig M. 2015.** Arbuscular mycorrhizal fungi reduce decomposition of woody plant litter while increasing soil aggregation. *Soil Biology and Biochemistry* **13**: 529–534.

**Li H, Bölscher T, Winnick M, Tfaily MM, Cardon ZG, Keiluweit M. 2021.** Simple plant and microbial exudates destabilize mineral-associated organic matter via multiple pathways. *Environmental Science & Technology* **55**: 3389–3398.

**Love MI, Huber W, Anders S. 2014.** Moderated estimation of fold change and dispersion for RNA-seq data with DESeq2. *Genome Biology* **15**: 550.

**Luthfiana N, Inamura N, Tantriani ST, Sato T, Oikawa A, Chen W, Tawaraya K. 2021.** Metabolite profiling of the hyphal exudates of *Rhizophagus clarus* and *Rhizophagus irregularis* under phosphorus deficiency. *Mycorrhiza* **31**: 403–412.

**McGuire KL, Treseder KK. 2010.** Microbial communities and their relevance for ecosystem models: decomposition as a case study. *Soil Biology and Biochemistry* **42**: 529–535.

**Miller RM, Jastrow JD. 2000.** Mycorrhizal influence on soil structure. In: Kapulnik Y, Douds DD, eds. *Arbuscular mycorrhizae: molecular biology and physiology*. Dordrecht, the Netherlands: Kluwer Academic, 3–18.

**Moni C, Rumpel C, Virto I, Chabbi A, Chenu C. 2010.** Relative importance of sorption versus aggregation for organic matter storage in subsoil horizons of two contrasting soils. *European Journal of Soil Science* **61**: 958–969.

**Nacoon S, Jogloy S, Riddech N, Mongkolthanaruk W, Kuyper TW, Boonlue S. 2020.** Interaction between phosphate solubilizing bacteria and arbuscular mycorrhizal fungi on growth promotion and tuber inulin content of *Helianthus tuberosus* L. *Scientific Reports* **10**: 4916.

**Nuccio E, Blazewicz S, Lafler M, Campbell A, Kakouridis A, Kimbrel JA, Wollard J, Vyshenska D, Riley R, Tomatsu A *et al.* 2022.** HT-SIP: a semi-automated stable isotope probing pipeline identifies interactions in the hyphosphere of arbuscular mycorrhizal fungi. *Microbiome* **10**: 199.

**Nuccio EE, Hodge A, Pett-Ridge J, Herman DJ, Weber PK, Firestone MK. 2013.** AMF alters soil bacterial community and N cycling. *Environmental Microbiology* **15**: 1870–1881.

**Oksanen J, Blanchet FG, Friendly M, Kindt R, Legendre P, McGlinn D, Minchin PR, O'hara RB, Simpson GL, Solymos P *et al.* 2019.** *Package 'vegan'. Community ecology package, v.2.9.* [WWW document] URL https://github.com/vegandevs/vegan [accessed 2 January 2020].

**Olsson PA, Wilhelmsson P. 2000.** The growth of external AM fungal mycelium in sand dunes and in experimental systems. *Plant and Soil* **226**: 161–169.

**Orwin KH, Kirschbaum MUF, St John MG, Dickie IA. 2011.** Organic nutrient uptake by mycorrhizal fungi enhances ecosystem carbon storage: a model-based assessment. *Ecology Letters* **14**: 493–502.

**Parks D, Chuvochina M, Waite D, Rinke C, Skarshewski A, Chaumeil PA, Hugenholtz P. 2018.** A standardized bacterial taxonomy based on genome phylogeny substantially revises the tree of life. *Nature Biotechnology* **36**: 996–1004.

**Parniske M. 2008.** Arbuscular mycorrhiza: the mother of plant root endosymbioses. *Nature Reviews Microbiology* **6**: 763–775.

**Paterson E, Sim A, Davidson J, Daniell TJ. 2016.** Arbuscular mycorrhizal hyphae promote priming of native soil organic matter mineralisation. *Plant and Soil* **408**: 243–254.

**Paul EA, Clark FE. 1989.** *Soil microbiology and biochemistry*. San Diego, CA, USA: Academic Press.

**Pett-Ridge J, Firestone MK. 2017.** Using stable isotopes to explore root–microbe–mineral interactions in soil. *Rhizosphere* **3**: 244–253.

**Pett-Ridge J, Weber PK. 2012.** NanoSIP: NanoSIMS applications for microbial biology. In: *Microbial systems biology: methods and protocols*. New York, NY: Springer US, 91–136.

**Pirozynski KA, Malloch DW. 1975.** The origin of land plants: a matter of mycotrophism. *Biosystems* **6**: 153–164.

**Qin H, Niu L, Wu Q, Chen J, Li Y, Liang C, Xu Q, Fuhrmann JJ, Shen Y. 2017.** Bamboo forest expansion increases soil organic carbon through its effect on soil arbuscular mycorrhizal fungal community and abundance. *Plant and Soil* **420**: 407–421.

**Quiroga G, Erice G, Aroca R, Chaumont F, Ruiz-Lozano JM. 2019.** Contribution of the arbuscular mycorrhizal symbiosis to the regulation of radial root water transport in maize plants under water deficit. *Environmental and Experimental Botany* **167**: 103821.

**R Core Team. 2017.** *R: a language and environment for statistical computing*. Vienna, Austria: R Foundation for Statistical Computing.

**Rillig MC. 2004.** Arbuscular mycorrhizae and terrestrial ecosystem processes. *Ecology Letters* **7**: 740–754.

**Rillig MC, Mardatin NF, Leifheit EF, Antunes PM. 2010.** Mycelium of arbuscular mycorrhizal fungi increases soil water repellency and is sufficient to maintain water-stable soil aggregates. *Soil Biology and Biochemistry* **42**: 1189–1191.

**Rillig MC, Mummey DL. 2006.** Mycorrhizas and soil structure. *New Phytologist* **171**: 41–53.

**Rillig MC, Wright SF, Eviner VT. 2002.** The role of arbuscular mycorrhizal fungi and glomalin in soil aggregation: comparing effects of five plant species. *Plant and Soil* **238**: 325–333.

**Rillig MC, Wright SF, Kimball BA, Pinter PJ, Wall GW, Ottman MJ, Leavitt SW. 2001a.** Elevated carbon dioxide and irrigation effects on water stable aggregates in a sorghum field: a possible role for arbuscular mycorrhizal fungi. *Global Change Biology* **7**: 333–337.

**Rillig MC, Wright SF, Nichols KA, Schmidt WF, Torn MS. 2001b.** Large contribution of arbuscular mycorrhizal fungi to soil carbon pools in tropical forest soils. *Plant and Soil* **233**: 167–177.

**Rodríguez-Caballero G, Caravaca F, Fernández-González AJ, Alguacil MM, Fernández-López M, Roldán A. 2017.** Arbuscular mycorrhizal fungi inoculation mediated changes in rhizosphere bacterial community structure while promoting revegetation in a semiarid ecosystem. *Science of the Total Environment* **584**: 838–848.

**Rorison B, Rorison IH. 1987.** Root hairs and plant growth at low nitrogen availabilities. *New Phytologist* **107**: 681–693.

**Ruth B, Khalvati M, Schmidhalter U. 2011.** Quantification of mycorrhizal water uptake via high-resolution on-line water content sensors. *Plant and Soil* **342**: 459–468.

**Sato T, Ezawa T, Cheng W, Tawaraya K. 2015.** Release of acid phosphatase from extraradical hyphae of arbuscular mycorrhizal fungus *Rhizophagus clarus*. *Journal of Soil Science and Plant Nutrition* **61**: 269–274.



© 2024 The Authors
*New Phytologist* © 2024 New Phytologist Foundation

14698137, 0, Downloaded from https://nph.onlinelibrary.wiley.com/doi/10.1111/nph.19560, Wiley Online Library on [03/04/2024]. See the Terms and Conditions (https://onlinelibrary.wiley.com/terms-and-conditions) on Wiley Online Library for rules of use; OA articles are governed by the applicable Creative Commons License

**Schmidt MWI, Torn MS, Abiven S, Dittmar T, Guggenberger G, Janssens IA, Kleber M, Kögel-Knabner I, Lehman J, Manning DAC *et al.* 2011.** Persistence of soil organic matter as an ecosystem property. *Nature* **478**: 49–56.

**Schüßler A, Schwarzott D, Walker C. 2001.** A new fungal phylum, the Glomeromycota: phylogeny and evolution. *Mycological Research* **105**: 1413–1421.

**See CR, Keller AB, Hobbie SE, Kennedy PG, Weber PK, Pett-Ridge J. 2022.** Hyphae move matter and microbes to mineral microsites: integrating the hyphosphere into conceptual models of soil organic matter stabilization. *Global Change Biology* **8**: 2527–2540.

**Smith SE, Read DJ. 2008.** *Mycorrhizal symbiosis.* Cambridge, UK: Academic Press.

**Smits MM, Herrmann AM, Duane M, Duckworth OW, Bonneville S, Benning LG, Lundström U. 2009.** The fungal–mineral interface: challenges and considerations of micro-analytical developments. *Fungal Biology Reviews* **23**: 122–131.

**Sokol N, Whalen ED, Jilling A, Kallenbach C, Pett-Ridge J, Georgiou K. 2022.** The global distribution of mineral-associated soil organic matter, and its formation and fate under a changing climate. *Functional Ecology* **36**: 1411–1429.

**Sollins P, Kramer MG, Swanston C, Lajtha K, Filley T, Aufdenkampe AK, Wagai R, Bowden RD. 2009.** Sequential density fractionation across soils of contrasting mineralogy: evidence for both microbial-and mineral-controlled soil organic matter stabilization. *Biogeochemistry* **96**: 209–231.

**Sollins P, Swanston C, Kleber M, Filley T, Kramer M, Crow S, Caldwell BA, Lajtha K, Bowden R. 2006.** Organic C and N stabilization in a forest soil: evidence from sequential density fractionation. *Soil Biology and Biochemistry* **38**: 3313–3324.

**Soudzilovskaia NA, van Bodegom PM, Terrer C, van't Zelfde M, McCallum I, McCormack ML, Fisher JB, Brundrett MC, de Sá NC, Tedersoo L. 2019.** Global mycorrhizal plant distribution linked to terrestrial carbon stocks. *Nature Communications* **10**: 1–10.

**Soudzilovskaia NA, van der Heijden MG, Cornelissen JH, Makarov MI, Onipchenko VG, Maslov MN, Akhmetzhanova AA, van Bodegom PM. 2015.** Quantitative assessment of the differential impacts of arbuscular and ectomycorrhiza on soil carbon cycling. *New Phytologist* **208**: 280–293.

**Spatafora JW, Chang Y, Benny GL, Lazarus K, Smith ME, Berbee ML, Bonito G, Corradi N, Grigoriev I, Gryganskyi A *et al.* 2016.** A phylum-level phylogenetic classification of zygomycete fungi based on genome-scale data. *Mycologia* **108**: 1028–1046.

**Strickland TC, Sollins P. 1987.** Improved method for separating light- and heavy-fraction organic material from soil. *Soil Science Society of America Journal* **51**: 1390–1393.

**Sulman BN, Moore JA, Abramoff R, Averill C, Kivlin S, Georgiou K, Sridhar B, Hartman MD, Wang G, Wieder WR *et al.* 2018.** Multiple models and experiments underscore large uncertainty in soil carbon dynamics. *Biogeochemistry* **141**: 109–123.

**Throckmorton HM, Bird JA, Monte N, Doane T, Firestone MK, Horwath WR. 2015.** The soil matrix increases microbial C stabilization in temperate and tropical forest soils. *Biogeochemistry* **122**: 35–45.

**Toljander JF, Artursson V, Paul LR, Jansson JK, Finlay RD. 2006.** Attachment of different soil bacteria to arbuscular mycorrhizal fungal extraradical hyphae is determined by hyphal vitality and fungal species. *FEMS Microbiology Letters* **254**: 34–40.

**Toljander JF, Lindahl BD, Paul LR, Elfstrand M, Finlay RD. 2007.** Influence of arbuscular mycorrhizal mycelial exudates on soil bacterial growth and community structure. *FEMS Microbiology Ecology* **61**: 295–304.

**Tome E, Tagliavini M, Scandellari F. 2015.** Recently fixed carbon allocation in strawberry plants and concurrent inorganic nitrogen uptake through arbuscular mycorrhizal fungi. *Journal of Plant Physiology* **179**: 83–89.

**Torn MS, Trumbore SE, Chadwick OA, Vitousek PM, Hendricks DM. 1997.** Mineral control of soil organic carbon storage and turnover. *Nature* **389**: 170–173.

**Treseder KK. 2016.** Model behavior of arbuscular mycorrhizal fungi: predicting soil carbon dynamics under climate change. *Botany* **94**: 417–423.

**Trumbore S. 2000.** Age of soil organic matter and soil respiration: radiocarbon constraints on belowground C dynamics. *Ecological Applications* **10**: 399–411.

**Wagg C, Bender SF, Widmer F, van der Heijden MG. 2014.** Soil biodiversity and soil community composition determine ecosystem multifunctionality. *Proceedings of the National Academy of Sciences, USA* **111**: 5266–5270.

**Wang ZG, Bi YL, Jiang B, Zhakypbek Y, Peng SP, Liu WW, Liu H. 2016.** Arbuscular mycorrhizal fungi enhance soil carbon sequestration in the coalfields, northwest China. *Scientific Reports* **6**: 1–11.

**Wei L, Vosátka M, Cai B, Ding J, Lu C, Xu J, Yan W, Li Y, Liu C. 2019.** The role of arbuscular mycorrhiza fungi in the decomposition of fresh residue and soil organic carbon: a mini-review. *Soil Science Society of America Journal* **83**: 511–517.

**Willis A, Rodrigues BF, Harris PJ. 2013.** The ecology of arbuscular mycorrhizal fungi. *Critical Reviews in Plant Sciences* **32**: 1–20.

**Wilson GW, Rice CW, Rillig MC, Springer A, Hartnett DC. 2009.** Soil aggregation and carbon sequestration are tightly correlated with the abundance of arbuscular mycorrhizal fungi: results from long-term field experiments. *Ecology Letters* **12**: 452–461.

**Wright SF, Franke-Snyder M, Morton JB, Upadhyaya A. 1996.** Time-course study and partial characterization of a protein on hyphae of arbuscular mycorrhizal fungi during active colonization of roots. *Plant and Soil* **181**: 193–203.

**Wu L, Wen C, Qin Y, Yin H, Tu Q, Van Nostrand JD, Yuan T, Yuan M, Deng Y, Zhou J. 2015.** Phasing amplicon sequencing on Illumina Miseq for robust environmental microbial community analysis. *BMC Microbiology* **15**: 1–12.

**Yuan MM, Kakouridis A, Starr E, Nguyen N, Shi S, Pett-Ridge J, Nuccio E, Zhou J, Firestone M. 2021.** Fungal-bacterial co-occurrence patterns differ between AMF and non-mycorrhizal fungi across soil niches. *MBio* **12**: 10–1128.

**Zeglin LH, Wang B, Waythomas C, Rainey F, Talbot SL. 2016.** Organic matter quantity and source affects microbial community structure and function following volcanic eruption on Kasatochi Island, Alaska. *Environmental Microbiology* **18**: 146–158.

**Zhang HS, Zhou MX, Zai XM, Zhao FG, Qin P. 2020.** Spatio-temporal dynamics of arbuscular mycorrhizal fungi and soil organic carbon in coastal saline soil of China. *Scientific Reports* **1**: 1–13.

## Supporting Information

Additional Supporting Information may be found online in the Supporting Information section at the end of the article.

**Fig. S1** Atom% $^{13}C$ in shoots, roots, sand mix, and soil mix in +AMF, −AMF, and $^{12}C$ microcosms.

**Methods S1** Detailed $^{13}C$ calculations.

**Table S1** Data used in statistical analyses.

**Table S2** Data used to calculate how much carbon ($^{13}C$ and total C) was transported by arbuscular mycorrhizal fungi into the no-plant compartment in +AMF microcosms.

**Table S3** Atom% $^{13}C$ of hyphae from NanoSIMS measurements for the 37 samples discussed in the main text.

**Table S4** Amplicon sequence variants that significantly increased or decreased in relative abundance in the soil mix (no-plant compartment) of +AMF microcosms.

Please note: Wiley is not responsible for the content or functionality of any Supporting Information supplied by the authors. Any queries (other than missing material) should be directed to the *New Phytologist* Central Office.

© 2024 The Authors
*New Phytologist* © 2024 New Phytologist Foundation



14698137, 0, Downloaded from https://nph.onlinelibrary.wiley.com/doi/10.1111/nph.19560, Wiley Online Library on [03/04/2024]. See the Terms and Conditions (https://onlinelibrary.wiley.com/terms-and-conditions) on Wiley Online Library for rules of use; OA articles are governed by the applicable Creative Commons License